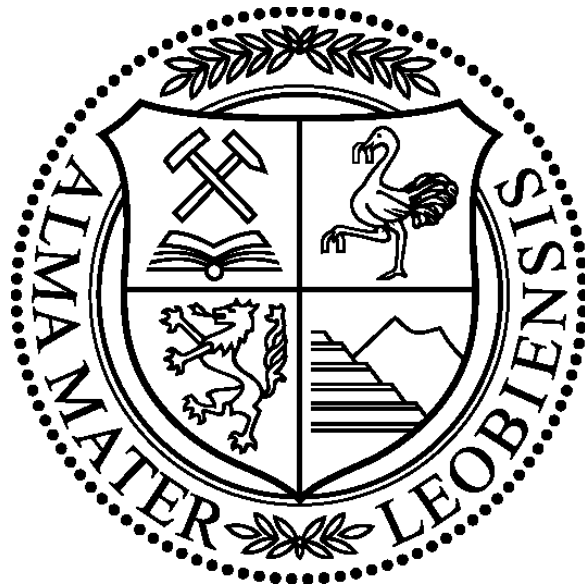


# Design and Experiment Concept of a Cutting Transport Simulation Apparatus for Solid Shape Investigation

*Master Thesis*

*Stefan Heinerman*

*Montanuniversität Leoben  
Department Petroleum Engineering  
Chair of Drilling and Completion Engineering*



*Supervised by:*

*Univ.-Prof. Dipl.-Ing. Dr.mont. Gerhard Thonhauser*

---

## EIDESSTATTLICHE ERKLÄRUNG

Ich erkläre an Eides statt, dass ich diese Arbeit selbständig verfasst, andere als die angegebenen Quellen und Hilfsmittel nicht benutzt und mich auch sonst keiner unerlaubten Hilfsmittel bedient habe.

## AFFIDAVIT

I declare in lieu of oath, that I wrote this thesis and performed the associated research myself, using only literature cited in this volume.

---

(Place, Date)

---

(Stefan Heinerman)

---

# ACKNOWLEDGMENTS

The author would like to thank the following:

Dipl.-Ing. Asad Elmgerbi and Dipl.-Ing. Christoph Thonhofer for their help, ideas and technical assistance during the whole project.

Special thanks to my family who made this study possible not only in financial terms, but also by moral support.

Not least the department of drilling and completion engineering at the Montanuniversität Leoben.

---

## ABSTRACT

Sufficient removal and transportation of solids generated during the drilling process is a major concern in any wellbore. Inefficiencies cause millions of dollars of direct, indirect and hidden costs for oil and gas companies in terms of increased bit wear, low *Rate of Penetration* (ROP), increased *Equivalent Circulation Density* (ECD), which may cause formation fracture and high torque and drag, possibly leading to mechanical pipe sticking. Problems related to poor cutting removal and transportation may in the worst case cause a loss of the wellbore.

The thesis provides an overview of previously developed models, including necessary assumptions made to predict and estimate cutting transportation efficiency. It points out the variations for vertical, inclined and horizontal sections of a wellbore and describes the key parameters that influence removal and transportation capabilities of solids and their controllability during the drilling process.

It also includes recommendations for the necessary equipment for the experimental setup, like the artificially produced solids, their characteristics and production, the transparent drilling fluid with all its properties and the design of a cutting transport simulation apparatus, which provides the opportunity to investigate the impact of the solids shape on transport and accumulation capacities amongst other factors.

Furthermore it discusses seven experiments, designed to investigate the impact of the cuttings shape on parameters like the particles slip velocity, the *Minimum Transport Velocity* (MTV) for desired flow patterns, the *Cutting Bed Height* (CBH) and the necessary duration of circulation with predefined flow rates to erode a cutting bed. The experimental data obtained with help of these experiments allow the validation of the advantages or disadvantages of both investigated shapes on removal and transport characteristics. Those results will further enable the adjustment of drilling parameters to optimize the overall drilling process.

---

## KURZFASSUNG

Die effiziente Beseitigung und der Transport von Bohrklein, das während des Bohrvorganges generiert wird, ist ein wichtiges Anliegen bei jeder Bohrung. Ineffizienz verursacht bei Öl- und Gasfirmen direkte, indirekte und versteckte Kosten in Millionenhöhe, sowohl durch einen erhöhten Verschleiß des Bohrmeißels und der damit verbundenen Verringerung des Bohrfortschritts, als auch durch eine Erhöhung der äquivalenten Zirkulationsdichte, die zu einem Aufbrechen der Formation führen kann. Des Weiteren kommt es zu einer Erhöhung der auftretenden Reibungskräfte, welche möglicherweise zu einem mechanischen Feststecken des Bohrstranges führen können. Probleme, im Zusammenhang mit unzureichender Entfernung und Transport des Bohrkleins, können im schlimmsten Falle zu einem Verlust des Bohrloches führen.

Die Arbeit liefert einen Überblick über zuvor entwickelte Modelle und nötige, getroffene Annahmen zur Vorhersage und Bestimmung der Effizienz des Bohrkleintransportes. Die Unterschiede, zwischen vertikalen, geneigten und horizontalen Sektionen eines Bohrloches werden hervorgehoben und die Schlüsselparameter, welche die Entfernungs- und Transportfähigkeit der Feststoffe beeinflussen, sowie deren Steuerbarkeit während des Bohrvorgangs, werden erläutert.

Sie beinhaltet ebenfalls Vorschläge für das benötigte Zubehör für den Versuchsaufbau, wie die künstlich erzeugten Feststoffe, deren Besonderheiten und Produktion, die transparente Bohrflüssigkeit mit den wichtigsten Eigenschaften. Anschließend wird das Design einer Simulationseinrichtung für Bohrkleintransport diskutiert, die unter anderem eine Untersuchung der Auswirkung der Bohrkleingeometrie auf den Transport und Ansammlungstendenzen ermöglicht.

Des Weiteren beinhaltet sie die Diskussion von sieben Experimenten, die konzipiert wurden um die Auswirkungen der Bohrkleinform auf mehrere Parameter, wie der Rutschgeschwindigkeit der Partikel, der minimalen

---

Transportgeschwindigkeiten für gewünschte Fließschemen, der Höhe des Bohrkleinbettes und der nötigen Zirkulationsdauer, die benötigt wird, um bei vorgegebener Fließrate ein Bohrkleinbett zu erodieren, zu untersuchen. Die Ergebnisse, die mit Hilfe dieser Experimente gewonnen werden, ermöglichen eine Überprüfung der Vor- oder Nachteile der beiden, in der Arbeit beschriebenen, Formen auf die Beseitigungs- und Transportfähigkeit. Des Weiteren ermöglichen diese Ergebnisse eine Anpassung der Bohrparameter um den gesamten Bohrprozess zu optimieren.

---

# TABLE OF CONTENTS

<b>ACKNOWLEDGMENTS.....</b>	<b>III</b>
<b>ABSTRACT.....</b>	<b>IV</b>
<b>KURZFASSUNG.....</b>	<b>V</b>
<b>TABLE OF CONTENTS .....</b>	<b>VII</b>
<b>LIST OF FIGURES .....</b>	<b>IX</b>
<b>LIST OF TABLES .....</b>	<b>XI</b>
<b>1 INTRODUCTION.....</b>	<b>1</b>
<b>2 FINDINGS OF PREVIOUS STUDIES .....</b>	<b>6</b>
2.1 Cutting Transport Overview .....	8
2.2 Key Parameters .....	14
2.3 Models and Correlations Review .....	22
<b>3 EXPERIMENTAL SETUP .....</b>	<b>32</b>
3.1 Artificial Cuttings .....	32
3.2 Fluid Properties .....	37
3.3 Solid Transport Apparatus Specification .....	50
<b>4 EXPERIMENTAL PROCEDURES AND OBJECTIVES.....</b>	<b>57</b>
4.1 General Parameters .....	57
4.2 TV - Experiment.....	61
4.3 CAFV/MAFV - Experiment .....	69
4.4 MTRV/MTSV - Experiment .....	74
4.5 CBH - Experiment .....	77
4.6 CBET - Experiment.....	81

---

4.7	SV - Experiment .....	85
4.8	MASV - Experiment .....	85
<b>5</b>	<b>CONCLUSION .....</b>	<b>89</b>
<b>6</b>	<b>FUTURE WORK .....</b>	<b>91</b>
	<b>NOMENCLATURE .....</b>	<b>92</b>
	List of Abbreviations .....	92
	List of Symbols .....	93
	<b>SI METRIC CONVERSION FACTORS .....</b>	<b>95</b>
	<b>REFERENCES .....</b>	<b>96</b>



---

## LIST OF FIGURES

Figure 1: First Version of the Flow Loop .....	1
Figure 1.2: Cutting Transport Key Variables and Controllability .....	3
Figure 2.1: Factors Affecting Hole Cleaning.....	6
Figure 2.2: Typical Mud Circulation System .....	8
Figure 2.3: Particle Diameter and Solids Removal Equipment .....	9
Figure 2.4: Stuck Pipe Causes in 1993 .....	10
Figure 2.5: Forces Acting on Particle in an Inclined Annulus.....	12
Figure 2.6: Force Directions for Vertical, Inclined and Horizontal Wellbore.....	12
Figure 2.7: Predetermined and Experienced Cutting Size Influence .....	16
Figure 2.8: Predetermined and Experienced Viscosity Influence.....	17
Figure 2.9: Predetermined and Experienced Mud Weight Influence.....	18
Figure 2.10: Influence of Inclination and ROP on MTV .....	19
Figure 2.11: Predetermined and Experienced ROP Influence .....	20
Figure 2.12: Pipe Eccentricity on Minimum Transport Fluid Velocity .....	22
Figure 2.13: Two-Layer Model Description .....	23
Figure 2.14: Three- Layer Model Description .....	24
Figure 3.1: Rule of Mixtures.....	34
Figure 3.2: Particle Sizes .....	36

---

Figure 3.3: Visualization of Flow Regime with Dye Tracers.....	38
Figure 3.4: Flow Regime Dependence on Shear Rate.....	39
Figure 3.5: Rheological Fluid Models.....	40
Figure 3.6: Shear Stress vs. Shear Rate Drilling Fluid 1.....	48
Figure 3.7: Shear Stress vs. Shear Rate Drilling Fluid 2.....	49
Figure 3.8: Shear Stress vs. Shear Rate Drilling Fluid 3.....	50
Figure 3.9: Flow Loop Schematic .....	51
Figure 4.1: Magnitude of Determined Velocities .....	60
Figure 4.2: Experiment Flow Chart .....	61
Figure 4.3: Mainly Stationary Bed and Partially Moving .....	70
Figure 4.4: Suspension Flow .....	70
Figure 4.5: Moving Cutting Bed .....	74
Figure 4.6: Cuttings Bed Perimeter.....	79

---

## LIST OF TABLES

Table 2.1: Sphericities for Various Particle Shapes .....	15
Table 3.1: Sandstone Specific Gravity.....	34

# 1 INTRODUCTION

Several authors stated in the past, that the cuttings shape has a big influence on removal, transportation and accumulation characteristics [1] [2]. However no major research projects have been conducted so far in that field. Therefore the objective was to develop and implement experiments to investigate the impact of the cuttings shape with an already existing flow loop, seen in Figure 1. The flow loop was designed by students in a course for teaching purpose to simulate cuttings transportation in order to improve the understanding of the solids behaviour in the annulus of the wellbore.



**Figure 1: First Version of the Flow Loop**

Since the existing flow loop does not fulfil the necessary prerequisites, the new objective was to develop experiments for solids shape investigation first and then

to design a cutting transport simulation apparatus for solid shape investigation with the necessary prerequisites and the necessary equipment to implement the designed experiments, such as artificially produced cuttings, a transparent drilling fluid and additional fluid tanks to name but a few. For cuttings shape investigations, it is necessary to artificially produce solids with uniform physical properties, such as same density, size and surface roughness, but different shapes. The density is chosen to be representative for a frequently encountered formation in the drilling process: sandstone.

Drill cuttings are generated at the bottom of the wellbore where the rotating bit crushes or shears off the formation below. The exact mechanism depends on the used bit, the type of formation itself as well as on various factors of the drilling process. Nowadays rotary drilling is the standard drilling method in the oil and gas industry. In the late 1980's directional drilling was revolutionised with help of positive-displacement mud motors, which made it possible to turn the drill bit independently from the rotation of the drill string. Before that, vertical drilling operations outnumbered horizontal and deviated drilling projects [3] [4].

With the development of directional drilling and increasing demand for *Extended Reach Drilling* (ERD) to face challenges like stricter environmental regulations, improving recovery from existing reserves smaller footprints and reducing costs, sufficient cutting transport is a major concern in any wellbore. The overall horizontal departure of the well divided by the total vertical depth defines an ERD ratio. If the ERD ratio is above two, the wellbore is classified as an extended-reach well [5]. As horizontal departure and measured depths increase, good hole cleaning and cuttings removal are crucial tasks maintained by the drilling fluid. They have to be monitored using real-time analysis of surface and down-hole measurements and need to be controlled properly during the whole drilling operation.

Poor borehole cleaning due to insufficient solids transportation and removal leads to deposition and accumulation of cuttings to so-called cutting beds in the annulus of the wellbore. An excessive concentration of solids in the well changes the fluid's rheological properties and prolongs the evaluated project time, caused by

problems as reduction in *Rate of Penetration* (ROP) due to inefficient cuttings removal, mechanical pipe sticking, increase in torque and drag, which may limit the reach which is necessary to hit the target, difficulties in casing or liner running jobs, wellbore stability problems, excessive over-pull on trips, lost circulation and increase of bit wear. Besides *Health, Safety and Environmental* (HSE) risks, the overall costs of the project rise and the profit decreases. Therefore the effects of key variables and parameters influencing hole cleaning efficiency need to be monitored, understood and controlled properly. Many investigations have been performed in the past decades to evaluate the impact of key factors controlling hole cleaning efficiency and transportation behavior.

Figure 1.2 graphically illustrates the influence and controllability in the field of major factors influencing cutting transport that have been extensively investigated and rated. Namely flow rate, hole size and angle, drill pipe eccentricity, fluid rheology, mud weight, ROP, density of the cuttings and other key variables in the drilling process.

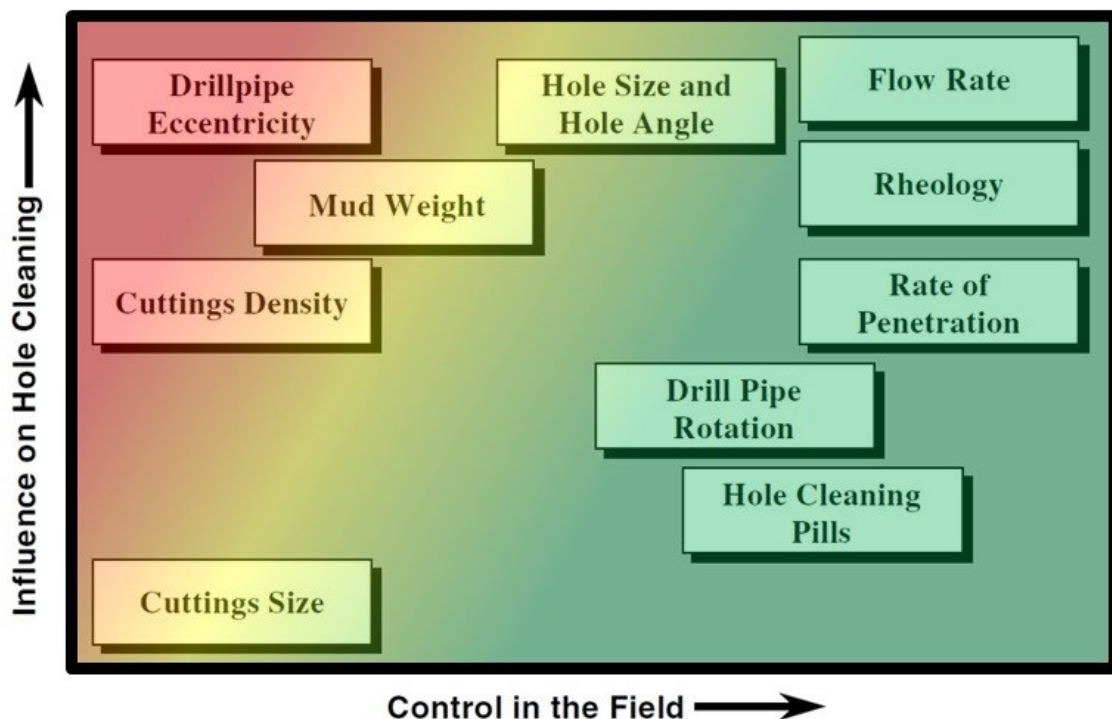


Figure 1.2: Cutting Transport Key Variables and Controllability [6] (Modified by the author)

The generated cuttings are removed and transported by the viscous forces of the drilling fluid. The ability of the fluid to transport solids in the annulus of the wellbore to the surface is in turn depending on many different factors. One of them, which has not been investigated and rated yet is the cuttings shape. The shape of the cuttings is a variable whose influence on transport efficiency, deposition and accumulation tendency is unsteady. Most equations are based on the assumption of spherical cuttings and provide correction factors as seen in Table 2.1 for solids slightly diverging from spherical. The shapes of the generated cuttings vary strongly depending on the drilling process and rock properties. Some of the influencing process parameters are the drill bit type and shape, the formation and the *Depth of Cut* (DOC). The DOC in turn is dependent on *Revolutions per Minute* (RPM) of the drill bit, the *Weight on Bit* (WOB) applied, the consolidation of the formation and the bit and cutter design. Rolling cutter bits drill the formation by crushing and fracturing rock fragments, while fixed cutter bits remove material by scraping or grinding due to the rotation of the drill bit. Depending on the shape and position of the chippings in the annular area, a different contact area and a varying momentum force of the drilling fluid is exerted on the particles, in vertical and in horizontal sections.

“The only practical way to estimate cutting transport or the slip velocity of cuttings is to develop empirical correlations based on experimental data.” [1]

Nowadays technical challenges require further improvements and therefore further investigations to fully understand the particle transport and accumulation behaviour in the different sections of a wellbore. This work is focused on the development of a new design for a cutting transport simulation apparatus. It provides an overview of the circulation system and the implemented equipment for handling and measuring certain parameters. Furthermore this work includes a meaningful step-by-step implementation of various experiments for the experimental investigation on the effect of the cuttings shape on transportation characteristics. The intention to design a flow loop for shape investigations is based on the statement of various authors, that the shape of the generated cuttings influences their transportation and accumulation behavior in the annular area of the wellbore [1] [2].

The parameters investigated with help of these experiments should provide highly diagnostic findings and options to investigate the influence of the particle shape on transport and accumulation characteristics. For first investigations two different shapes of artificially produced cuttings are described, which are circulated with help of a transparent drilling fluid to deliver observable and comparable results. Since the diameters of the flow loop are not in full-scale, it is necessary to downscale the size of the artificial cuttings. Therefore a scale factor is derived according to the geometric similarity model which is applicable for structures having the same shape [7]. The annular region can be observed due to a transparent outer pipe with an *Inside Diameter* (ID) of 70 mm and an inner pipe with an *Outside Diameter* (OD) of 40, 50, or 60 mm. The various proposed experiments make it possible to determine key factors, which were also used by former investigators. These include the *Minimum Transport Velocities* (MTV) to provide a desired mode of movement through the annulus, the *Critical Transport Velocities* (CTV), below which the solids way of movement is undesirable and their tendency to deposition and accumulation to so-called cutting beds is high, the cutting slip velocity, the *Cutting Bed Height* (CBH) and last but not least the erosion tendencies of cutting beds. Understanding the impact of key parameters influencing cutting transportation will lead to an improvement of the overall drilling process in term of energy efficiency, wellbore stability and time management, due to an improved drilling process. Knowing the advantages or disadvantages of the cuttings shape on transportation characteristics leads to an optimization of circulation practices during drilling and helps to reduce flat time, lost time and invisible lost time in the overall project.



## 2 FINDINGS OF PREVIOUS STUDIES

In the past decades substantial experimental, empirical investigations and sensitivity analysis have been performed to predict the impact of various parameters on cutting transport and hole cleaning for the vertical, inclined and horizontal sections of a wellbore. A big effort of research has been carried out by many laboratories and universities to investigate the physical mechanism of different phases flowing in a pipe and in the annular area between two pipes. This chapter provides a summary of previously developed models and correlations, used to estimate and predict hole cleaning efficiency. It lists the key factors that have the highest impact on cuttings removal and transportation. Furthermore it points out the parameters most commonly used in models and correlations for efficiency determination. Additionally, further factors influencing solids removal and transportation efficiency and their close connection with each other can be seen in Figure 2.1.

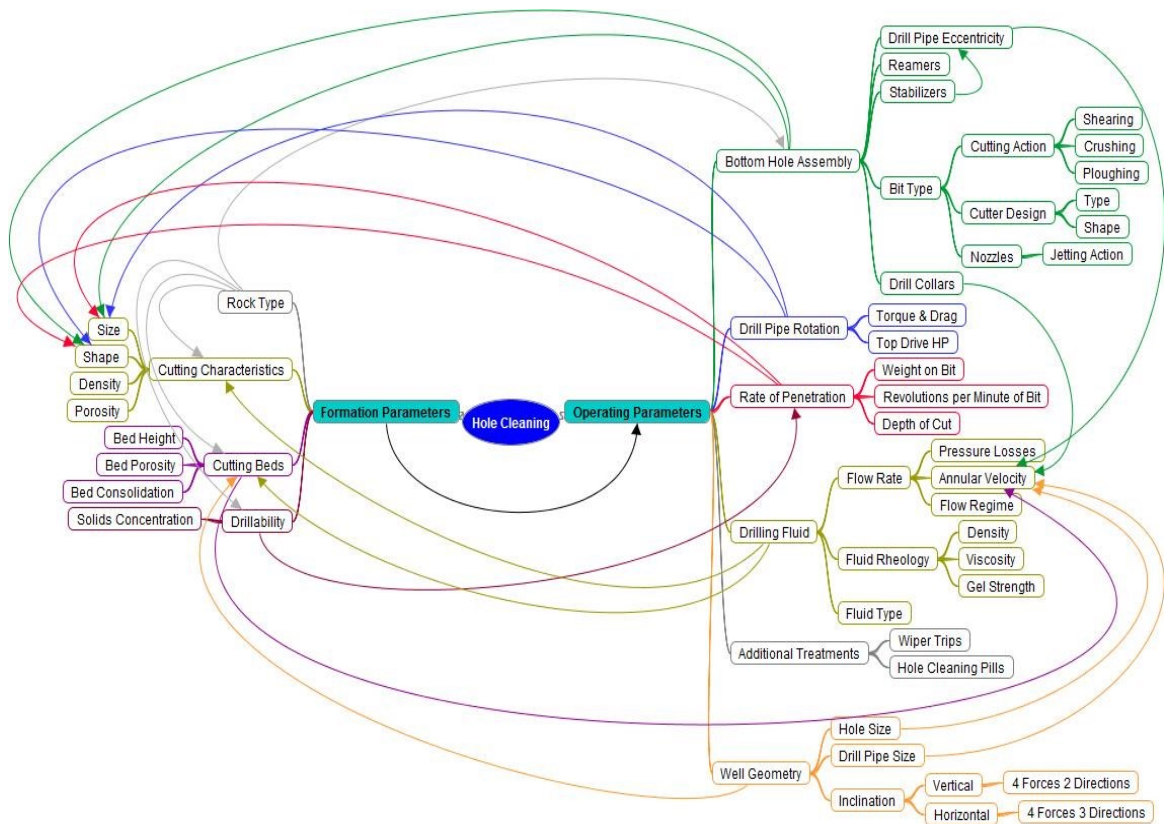


Figure 2.1: Factors Affecting Hole Cleaning

Figure 2.1 shows that the formation parameters as well as the operating parameters can be categorized in driving and responsive parameters. Driving parameters are the ones, which have a big influence on the responsive parameters. The coherence between driving and responsive parameters is illustrated by colored arrows. Proper handling of the driving parameters determines the responsive parameters and hence provides improved control on the hole cleaning efficiency.

As seen in Figure 2.1 the major driving parameter is the used *Bottom Hole Assembly* (BHA), since it is the origin of most of the arrows. Including drill bit type, cutter design and additional tools implemented in the drill string which may cause restrictions in the annular area or even change the generated cuttings shape and size while travelling upwards in the annulus. The BHA in turn is strongly affected by the rock type. Further examples for driving parameters are the drill pipe rotation, the *Rate of Penetration* (ROP) and the drilling fluid.

One of the most affected parameters is the *Annular Flow Velocity* (AFV) which in turn, combined with the wellbore geometry, has a major impact on the formation of cutting beds. Due to interfacial slip the cuttings generated at the bottom of the wellbore travel to the surface at a different velocity than the drilling fluid. To determine the cutting transport efficiency in the wellbore correctly, it is necessary to estimate the velocities of the different phases which are present in the annulus. The velocities are a function of the flow rate, the cross-sectional area and are dependent on the friction acting on the fluid as well as on the solids and on the interfacial forces between the solids.

The following section provides a short overview of the crucial task of cutting removal and transportation from the bottom of the wellbore to the surface.

## 2.1 Cutting Transport Overview

In terms of process observation the main principle of cutting transport remains the same for every wellbore. A mud pump, mostly a reciprocating piston pump, is used on surface to circulate the drilling fluid down through the hollow drill string and the bit nozzles, whereby the cutters of the bit and the bottom of the wellbore are cleaned from cuttings. The generated cuttings are lifted from the bottom of the wellbore up to the surface by the viscous forces of the drilling fluid. Figure 2.2 shows a schematic of a typical fluid circulation system used for cutting removal and transportation.

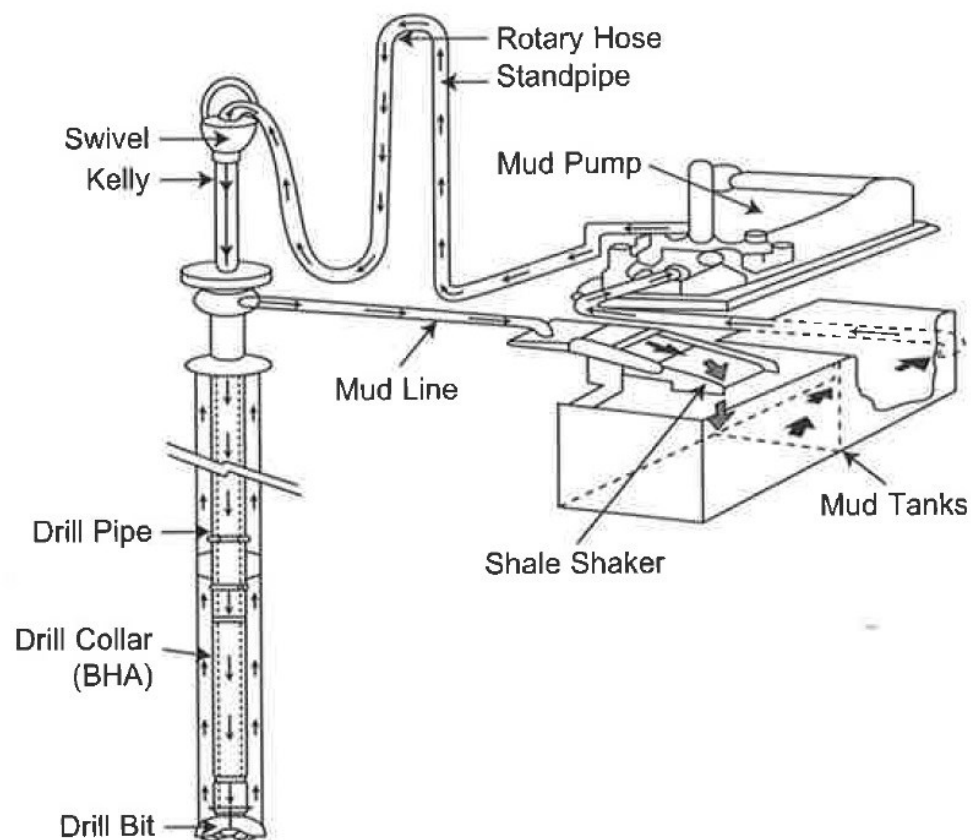


Figure 2.2: Typical Mud Circulation System ( [8], p.4)

The cuttings travel to surface in the annular region of the wellbore, between the borehole wall and the drill string. They get removed from the drilling fluid by solid-removal equipment in order to retain the very accurately predetermined fluid rheology. To remain in control of wellbore stability and well costs, the quantities and types of solids in the drilling fluid must be audited properly. Figure 2.3 shows the commonly used equipment for a given particle size distribution and the ideal order of placement for the different equipment used.

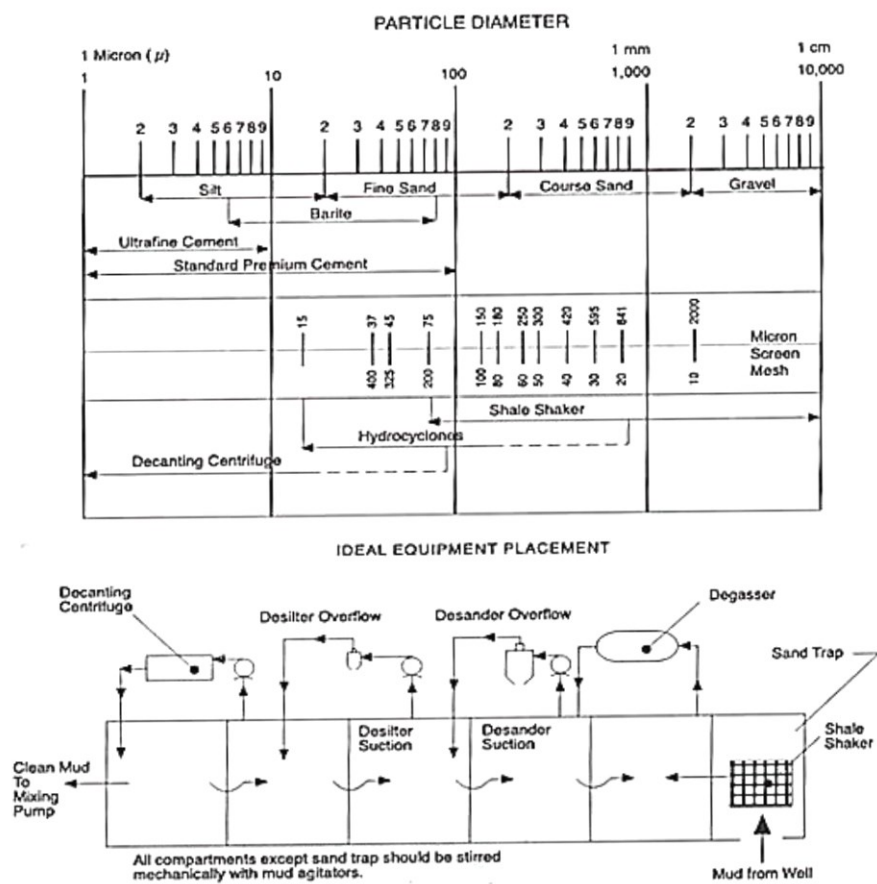


Figure 2.3: Particle Diameter and Solids Removal Equipment [9]

A high concentration of small sized solids present in the drilling fluid influences the fluid's mechanical and chemical properties as viscosity, gel strength, density, filter-cake quality, filtration control and others. An excessive annular cuttings concentration increases the mud weight and may cause pressures that fracture the

formation. Therefore the right removal equipment must be chosen precisely. In general, independent of the size of the cuttings, insufficient particle removal causes major problems in drilling activities worldwide. Even before the development of directional drilling and *Extended Reach Drilling* (ERD), inefficient cuttings removal and transportation was a major problem for drilling engineers to deal with. According to Hopkins *et al.* (1995), who investigated the reasons for stuck pipe, including logging tools and casings in Netherlands, around fifty percent of the encountered problems were related to poor hole cleaning and wellbore instability, as seen in Figure 2.4. With increased focus on solids removal equipment and techniques, fewer problems were observed in the following years. Differential sticking was another major reason causing stuck pipe mainly across reservoir sections in small hole sizes [10].

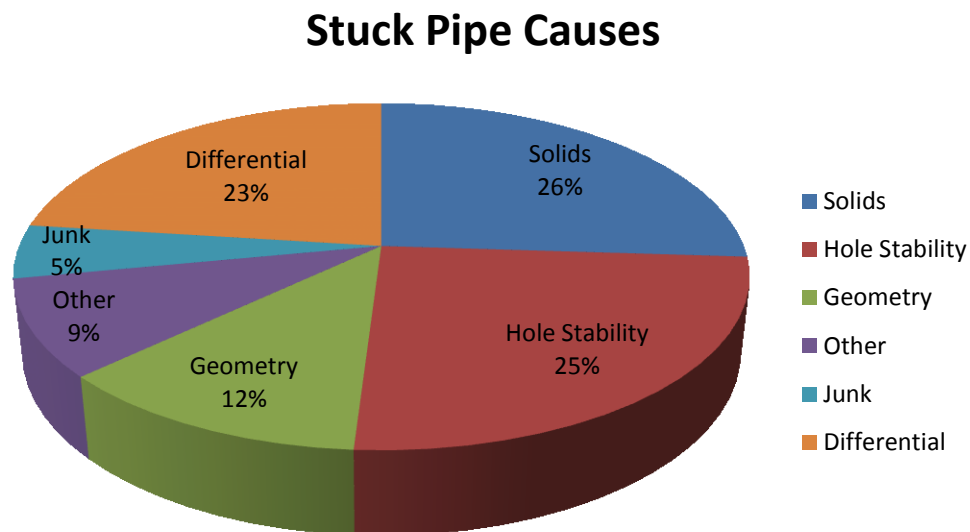


Figure 2.4: Stuck Pipe Causes in 1993 [10]

There is a broad variety of additives and drilling fluids available. The selection of drilling fluids is mainly based on the type of formation being drilled, ecological and environmental considerations, the temperature range, the necessary hydrostatic pressure and the permeability of the surrounding formation. Some of the drilling

fluid additives are weighting agents, fluid-loss-control additives, lost-circulation materials, surfactants or surface-active agents and various other additives [11].

The main functions of the drilling fluid are:

- Remove the generated rock fragments beneath the drill bit, to reduce bit wear and maintain high value of ROP.
- Transmit the hydraulic horsepower to the bit.
- Transport the cuttings to the surface where they are removed from the liquid with help of solids removal equipment to maintain the desired properties.
- Exert enough hydrostatic pressure to maintain wellbore pressure above the pore pressure, to prevent influx of formation fluids or gas into the wellbore, but below the formation fracture pressure to avoid fracturing of the surrounding formation.
- Reduce torque and drag, cool and lubricate the bit and drill string.
- Create an impermeable layer, surrounding the newly drilled formation, called filter cake, for fluid-loss control.

However the evaluation of cutting transport behavior and efficiency within a wellbore has to be separated into three different sections. Hence the net force direction acting on the rock fragments in the fluid stream is changing strongly with changing inclination. The flow direction of the cutting is subjected to many forces, such as buoyancy, gravity, inertia, drag, friction and interparticle forces. Figure 2.5 shows the main forces acting on a generated cutting as it is transported through an inclined annulus. With changing inclination the acting forces remain the same, but the direction of the dominating force varies [2].

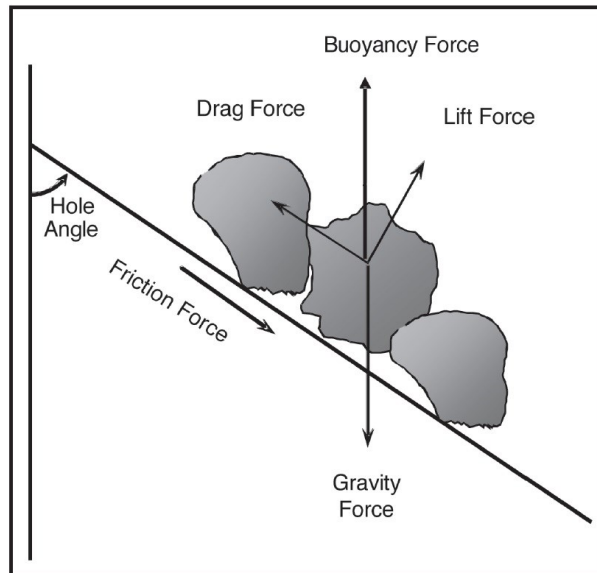


Figure 2.5: Forces Acting on Particle in an Inclined Annulus ([2], p.172)

Figure 2.6 illustrates how the force directions vary within vertical, inclined and horizontal sections of a wellbore.  $F_B$  represents the buoyancy force,  $F_R$  the friction force,  $F_G$  the gravity force and  $F_D$  the drag force.

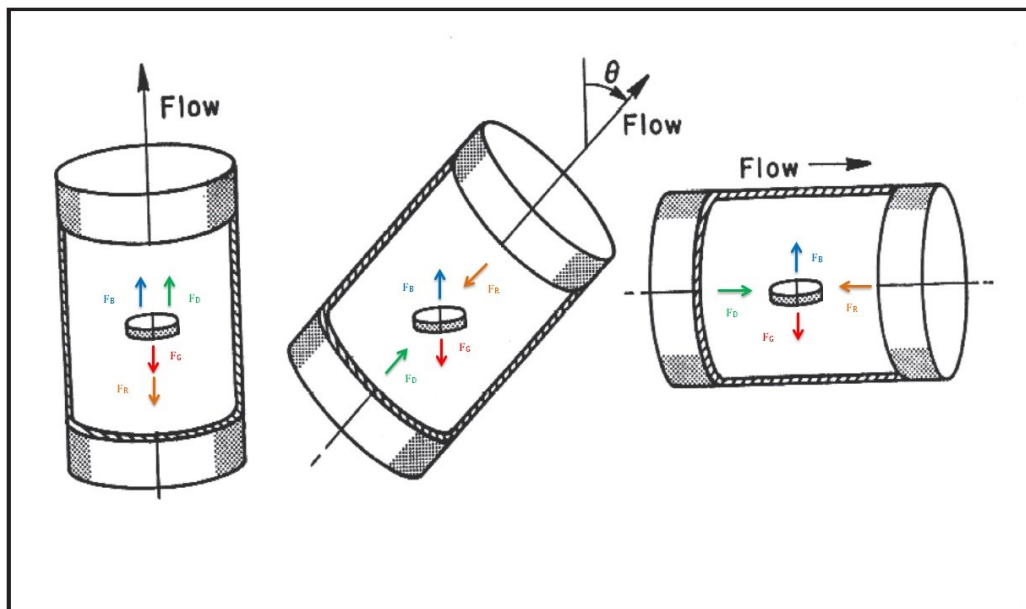


Figure 2.6: Force Directions for Vertical, Inclined and Horizontal Wellbore ([2], p.173) (Modified by the author)

### **Vertical and near vertical wellbores**

Gravity induces the solids to slip through the drilling fluid. In simple terms, there are two main force directions in vertical wellbores as seen in Figure 2.6, neglecting the interfacial forces between the particles themselves. There is a positive upward force, caused by the momentum of the fluid and the buoyancy force and a negative downward force, caused by the force of gravity acting on the cuttings and the friction force. For vertical wellbores the cuttings slip velocity concept can be used to determine the necessary flow rate to achieve sufficient hole cleaning in vertical wellbores. The cuttings transport velocity is a function of the annular velocity of the fluid and the solids slip velocity and can be expressed with equation (1).

$$V_T = V_a - V_{sl} \quad (1)$$

Different correlations are provided by different authors in various books to determine the particles slip velocity in Newtonian and non-Newtonian fluids, for static as well as for dynamic conditions [2] [11] [12]. Since the cross-sectional area remains approximately the same and no formation of cutting beds is present, the determination of an average annular velocity, based on the cuttings slip velocity is expedient. In horizontal sections on the other hand, the formation of beds can cause a reduction in the *Open Flow Area* (OFA) and thereby an increase in flow velocities.

### **Inclined and horizontal wellbores**

In high-angle and horizontal wells cuttings settle faster through the drilling fluid due to the changed net force directions along the bottom of the wellbore, forming a cutting bed. In contrast to vertical wells the positive upward force is strongly reduced, because the direction of the fluid's viscous forces is now shifted to horizontal and only buoyancy forces the solids in upward direction.



The use of an average transport velocity in terms of a cutting rise velocity to evaluate cutting transport efficiency as used for vertical wellbores is not suitable in inclined and horizontal wellbores, simply because of the formation of cutting beds. The formation of cutting beds cause a reduction in the annular cross-sectional area which in turn leads to an increase in velocities, both of the remaining cuttings in suspension and the drilling fluid. Experiments have shown that the use of the theoretical transport ratio as used for cutting slip velocity concept is limited to vertical wellbores.

Not only the generated cuttings tend to settle, also the barite, used in drilling fluids to achieve the necessary density to maintain well control, tends to deposit on the lower side of the wellbore. Therefore specialized fluid formulations and a different concept to determine hole cleaning efficiency are required for high-angle and horizontal wellbores, like a *Minimum Transport Velocity* (MTV) concept.

## 2.2 Key Parameters

Numerous factors have an impact on cuttings removal and transportation efficiency. Many of them influence the drilling fluids ability to remove and transport the generated cuttings through the annular area of the wellbore.

### **Size and shape of cutting**

Many investigations have been performed in the past to evaluate the impact of the cutting size on transportation characteristics. For the cuttings shape however, only few investigations have been performed and sphericity corrections have been derived for different shapes of solids, as for cubes, prisms and cylinders. This enables us to obtain average values for the slip velocity and other factors, instead of realistic values. A sphere's surface area divided by the surface area of a differently shaped particle with the same volume as the sphere is defined to be the

sphericity of the particle. Sphericity values for different particle shapes are available in Table 2.1 [11].

<u>Shape</u>	<u>Sphericity</u>
Sphere	1.0
Octahedron	0.85
Cube	0.81
<b>Prism</b>	
$l \cdot l \cdot 2l$	0.77
$l \cdot 2l \cdot 2l$	0.76
$l \cdot 2l \cdot 3l$	0.73
<b>Cylinders</b>	
$h = r/15$	0.25
$h = r/10$	0.32
$h = r/3$	0.59
$h = r$	0.83
$h = 2r$	0.87
$h = 3r$	0.96
$h = 10r$	0.69
$h = 20r$	0.58

**Table 2.1: Sphericities for Various Particle Shapes( [12], p.172)**

According to the experimental results provided by Larsen *et al.* (1997), smaller sized particles require a higher flow rate to reach the minimum necessary transport fluid velocity for proper hole cleaning as seen in Figure 2.7 [13].

Many authors stated that also the cutting shape has a big impact on their transportation behavior and that solids with irregular shape in a laminar flow regime are additionally subjected to a torque effect, but so far only a few investigations have been carried out [1] [2].

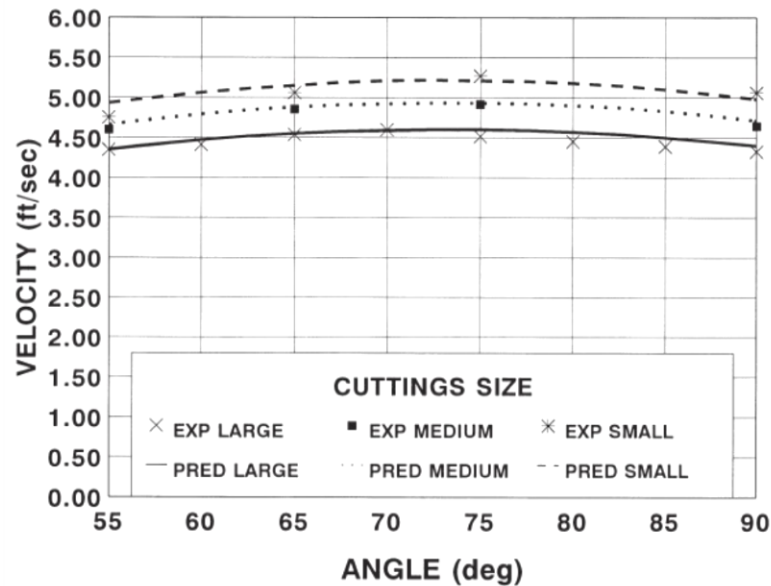


Figure 2.7: Predetermined and Experienced Cutting Size Influence [13]

### Drill pipe rotation

In vertical wellbores the rotation of the *Drill Pipe* (DP) with high revolutions per minute, exerts a centrifugal force on the cuttings. This causes the particles to permanently change their location, which is advantageous especially for already deposited and accumulated solids. Furthermore the centrifugal effect forces the cuttings to move towards the outer side of the annulus [1] [14]. This effect of DP rotation is even bigger for a small annular area, as encountered in slim hole drilling. In conventional horizontal wellbore sections this effect is reduced due to the increased annular area and because gravity acts against the centrifugal force. Additionally the rotation of the DP causes turbulences in the annular area, which is recommended for hole inclinations from 55 to 90 degrees.

### Fluid rheological properties and flow regimes

One of the main parameters influencing cutting transportation is the drilling fluids rheology. The mud weight and the viscosity are the properties which affect hole cleaning the most [4]. Malekzadeh *et al.* (2011) states, that for vertical wellbores

an increase of the fluids *Plastic Viscosity* (PV) and *Yield Point* (YP) decrease the minimum necessary velocity for efficient cuttings removal. But for high angles of inclination and horizontal wellbores an increase in PV and YP cause an increase of the minimum necessary velocity [15]. Additionally Larsen *et al.* (1997) found out that for high-angle wellbores, low-viscosity drilling fluids, or water, provide better hole cleaning, because the fluid velocity necessary to cause turbulent flow in the annulus is lower. Figure 2.8 shows the difference in minimum transport fluid velocities between water and a drilling fluid with a yield point between 24 and 26 lbf/100 ft<sup>2</sup> and a plastic viscosity between 24 and 27 centipoise.

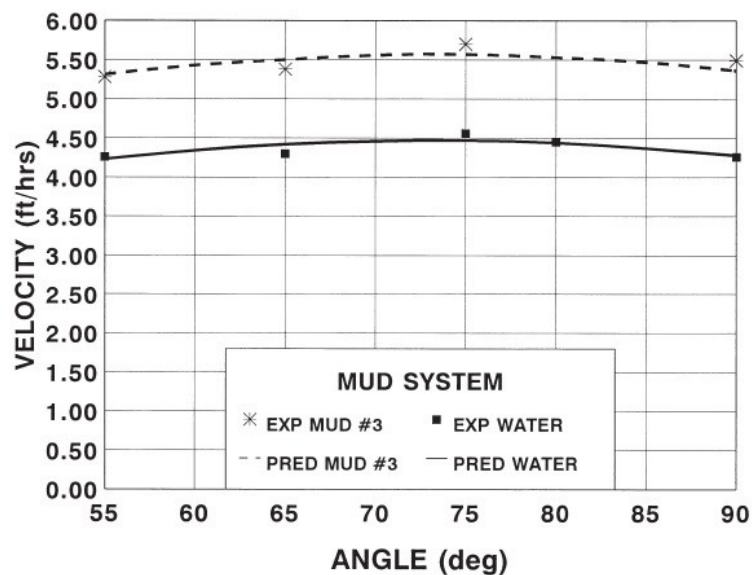


Figure 2.8: Predetermined and Experienced Viscosity Influence[13]

Also Mohammadsalehi *et al.* (2011) stated that clear water as a drilling fluid would be most efficient due to the low flow rate necessary to provoke turbulent flow in the annulus, which has shown best hole cleaning efficiency [4].

Furthermore the experimental results showed that if the fluids viscosity and yield point are kept constant and only the muds density is increased, the solids transportation efficiency is improved [13]. Figure 2.9 shows that the necessary minimum fluid velocity is lower for mud number 4 with a density of 11 lbm/gal,

than for mud number 2 with 8,65 lbm/gal. However, the mud density is never increased to improve hole cleaning, since an increase in mud weight decreases the ROP and thereby increases the overall drilling costs [4].

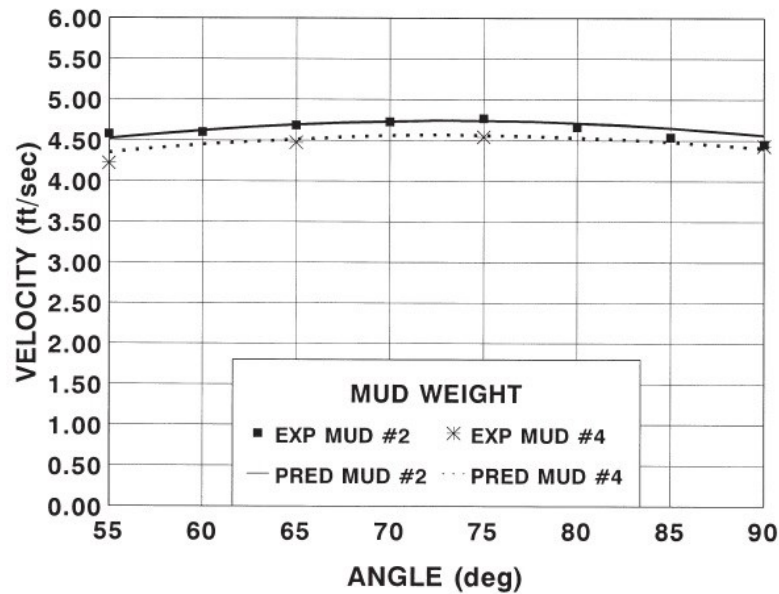


Figure 2.9: Predetermined and Experienced Mud Weight Influence [13]

### **Inclination**

Tomren *et al.* (1986) stated that with increasing hole angle the bed thickness and the cuttings concentration increase gradually. The formation of cutting beds is significant for hole inclinations above 40 degrees even for high flow rates. Above 60 degrees the bed thickness remains fairly the same. This means the interval from 40 to 60 degrees is worst for hole cleaning [14] [16].

Below hole inclinations of 30 degrees from vertical the cuttings stay in suspension and no formation of beds can be observed [17]. Hopkins *et al.* (1995) stated that there were clear indications that at hole angles above 30 degrees more wellbore problems occur. Especially the hole inclinations in the range between 40 and 60 degrees from vertical are very difficult to clean and require special procedures and alertness to avoid excessive cutting bed formation [10]. When the fluid flow is

stopped at higher angles, especially between 35 and 55 degrees, solid particles deposit on the lower side of the wellbore and cutting beds tend to slide and tumble downwards. For angles between 60 and 90 degrees the cuttings bed height remains nearly the same, also without circulation [11] [18].

Therefore it is necessary to estimate hole cleaning in horizontal and highly inclined sections in terms of a MTV instead of simply using the cuttings slip velocity without any correlations. The MTV is the necessary velocity to maintain an upward movement of the generated cuttings and to avoid deposition or accumulation of solids in the wellbore.

### **Rate of penetration**

A further major parameter influencing cutting transport efficiency is the rate of penetration. It directly influences the cuttings concentration in the wellbore and has to be calibrated to the other parameters like flow rate, *Revolutions per Minute* (RPM) and inclination of the wellbore. The higher the amount of cuttings generated at the bottom of the well due to high ROP, the higher the minimum necessary velocity and therefore the higher the required flow rate for sufficient solids removal as seen in Figure 2.10 [15].

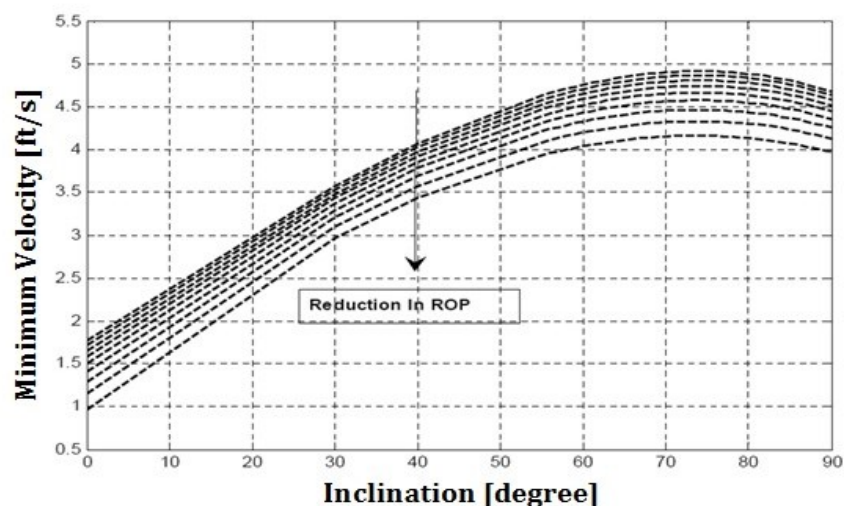


**Figure 2.10: Influence of Inclination and ROP on MTV [15]**

Larsen *et al.* (1997) also stated that an increase in cutting concentration due to an increase in ROP is directly linked with an increase of the necessary minimum transport velocity to achieve sufficient hole cleaning and provide similar results as illustrated in Figure 2.11 [13].

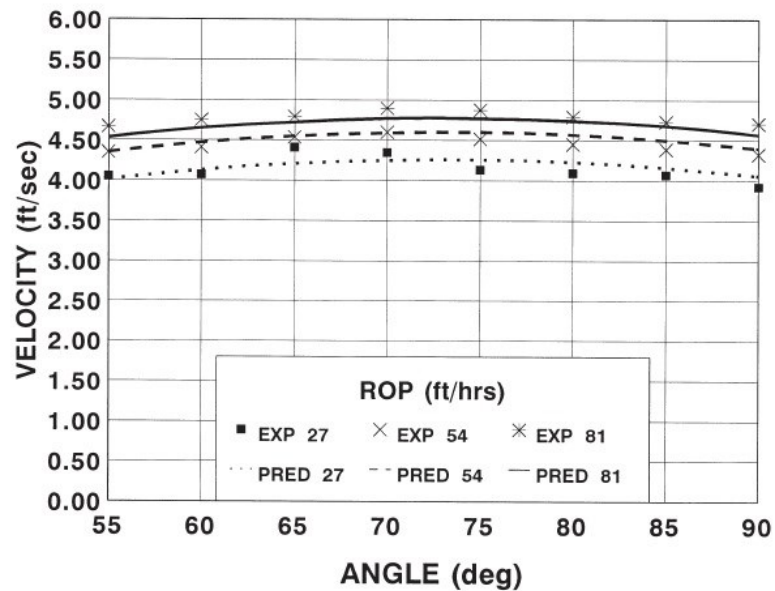


Figure 2.11: Predetermined and Experienced ROP Influence [13]

### Annular mud velocity

One of the most effective parameters for all cases influencing cuttings transportation is the flow rate, in other words the drilling fluids annular velocity. The reason for that is that the flow rate is easy to control and has a major influence on transportation characteristics. With an increase in flow rate the tendency of solids accumulating on the lower side of the annulus and forming a cutting bed is decreased, due to the higher shear stress exerted on the surface of the cuttings bed. However the upper limit of the flow rate is determined by the available hydraulic rig power, the maximum allowable *Equivalent Circulation Density* (ECD) and the sensitivity of the open hole section to erosion [4]. The largest necessary flow rate to provide sufficient hole cleaning may already increase the ECD in the horizontal or inclined section causing fracturing of the formation or borehole

breakouts [19]. The flow rate exerted by the mud pump induces strongly varying velocities over the whole wellbore. Firstly it causes different phase velocities, due to interfacial slip between the solids and the fluid. Secondly the velocities change due to changes in the annular cross-sectional area, like restrictions caused by drill string components such as reamers, stabilizers and tool joints, or due to the formation of cutting beds. Furthermore the fluid velocity varies from zero at the walls to a maximum in the center of the annular area. The flow rate is a major parameter affecting the flow regime present in the annulus. In general a turbulent flow caused by a high flow rate is most effective in terms of cutting transportation and removal, because the cuttings are carried more effectively and the formation of cutting beds is reduced. The flow rate and the velocity are the main factors influencing the cutting transport and hole cleaning efficiency and mainly set the limits to the drilling process.

### **Drill pipe eccentricity**

Drill pipe eccentricity has a big influence on cutting transportation [4]. According to the experimental study performed by Larsen *et al.* (1997), an eccentric drill pipe with a smaller annular area on the bottom causes higher viscosity muds to divert more flow from the bottom of the DP, where more solids are present, to the top [13]. As seen in Figure 2.12 a positive DP eccentricity, representing a pipe in the horizontal section resting on the tool joints and thereby decreasing the lower annular area, reduces the necessary annular velocity for cutting removal significantly.



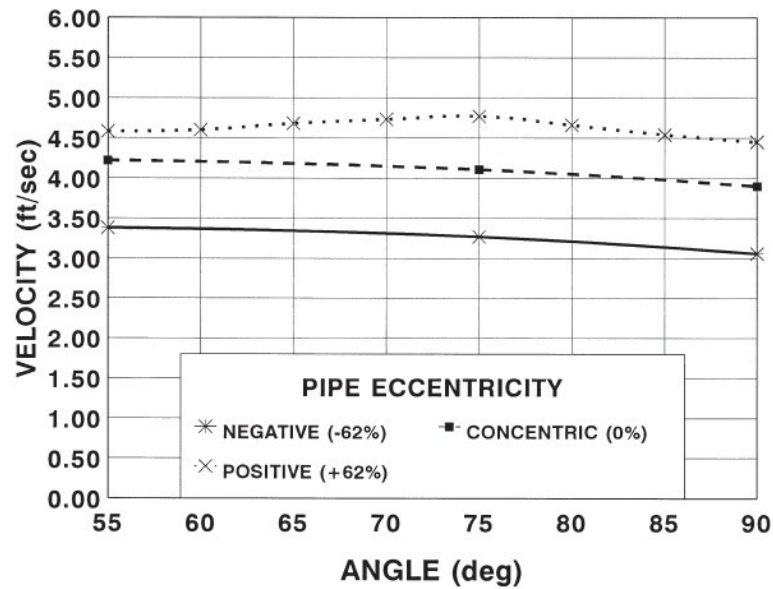


Figure 2.12: Pipe Eccentricity on Minimum Transport Fluid Velocity [13]

## 2.3 Models and Correlations Review

As in former times most wells were vertical, first investigations were focused on determining the cuttings terminal transport velocity for single phase fluids, which was enough to solve some of the problems related to poor cutting transport efficiency. But with increasing interest in directional and horizontal wellbores, investigations were shifted to mechanistic models and experimental approaches for explaining the phenomenon of cutting transport for all ranges of inclination [20].

Since then numerous methods, models and correlations have been developed for the interpretation and prediction of cutting transport efficiency, including one-layer models for vertical flow as well as two-layer and three-layer models for horizontal and inclined flow. Also dimensionless models have been developed to predict hole cleaning efficiency [20].

Figure 2.13 shows a two-layer model for solid transportation in the horizontal section. In the two-layer models the upper layer consists of a two-phase solid-

liquid suspension and the lower layer is made up of deposited cuttings forming a cutting bed [19] [21] [22] [23].

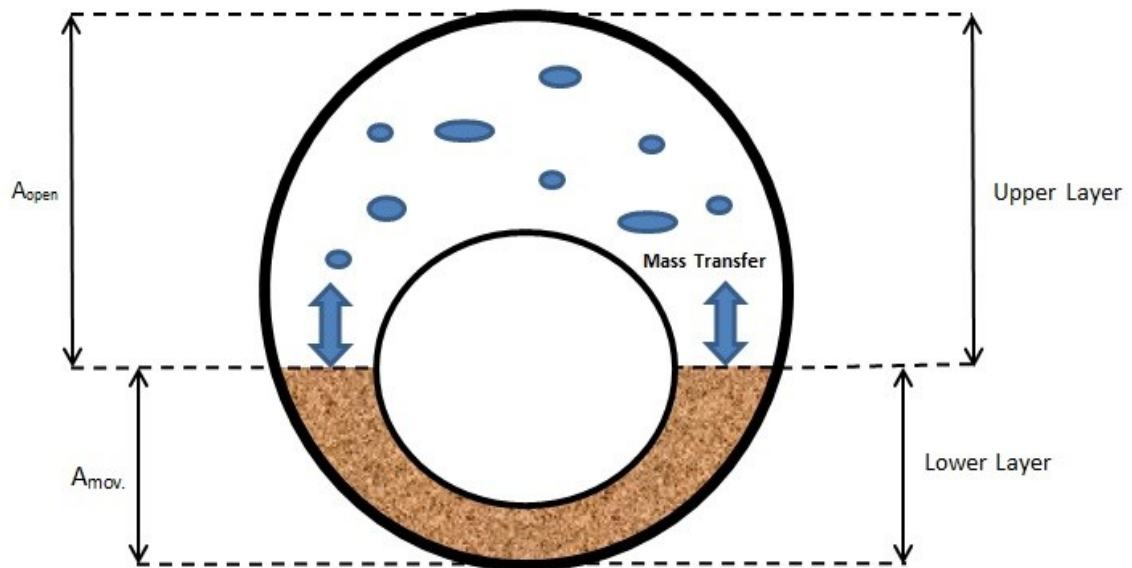


**Figure 2.13: Two-Layer Model Description**

In contrast to the two-layer models, the three-layer models consider a liquid phase on top, a suspension layer in the middle and a cuttings bed layer on bottom [24]. However other three-layer models, as seen in Figure 2.14, consist of a solid-liquid suspension, a moving layer in the middle and a stationary cuttings bed layer on bottom [25] [26].

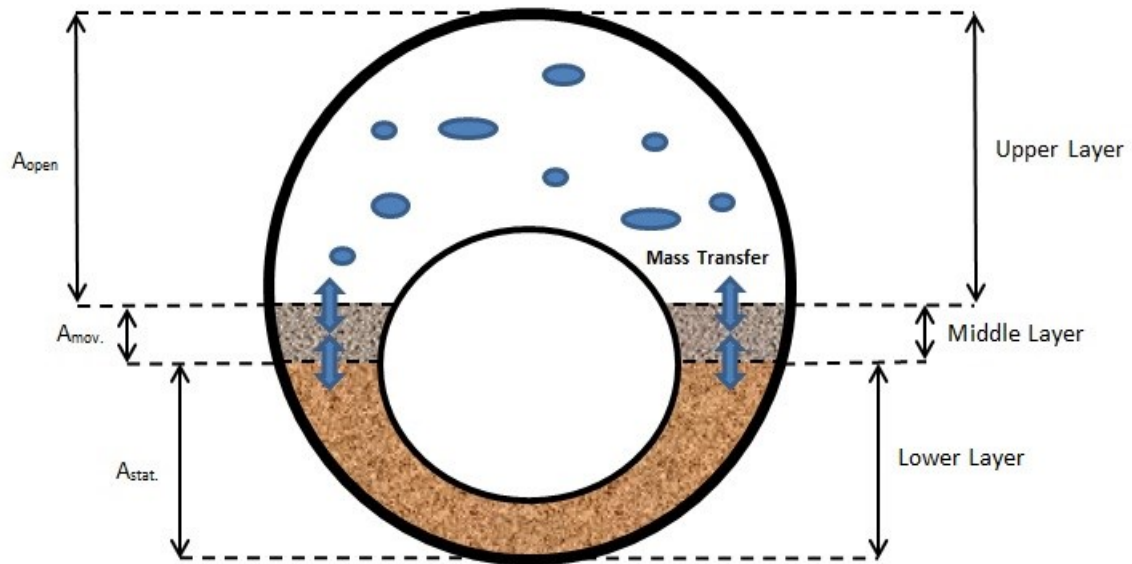


**Figure 2.14: Three- Layer Model Description**

Where  $A_{open}$  defines the OFA for liquid or suspension flow,  $A_{mov}$  is the area of a moving cutting bed and  $A_{stat}$  is the area of a stationary cutting bed.

Numerous models to predict cuttings removal in horizontal sections work with a so called “*Critical Transport Velocity*” (CTV) and are based on equations like the mass conservation equation (2), the momentum equation (3) and Stokes law (4) to describe the mass and momentum exchange between the different layers, co-existing in inclined and horizontal wellbores [19] [22] [23] [26] [27].

A common problem with the existing models is that several assumptions were made for simplification of the complexity of the real process [21] [28]. Common assumptions for the models are laminar flow conditions, the shape of the cuttings is assumed to be spherical or near spherical, including uniform sized particles, incompressibility of solids and liquids and the rheology of the drilling fluid follows the power law model. Furthermore the slip velocities of the solids are not considered or just simplified. Another major assumption is the steady-state transportation of the drill cuttings through the annulus [23] [26] [27].

$$\frac{\partial}{\partial t}(A_o C) + \frac{\partial}{\partial x}(A_o C u) = -\frac{A_o \Delta s}{\rho} \quad (2)$$

$t$  ... time [s]

$\Delta s$  ... change of mass between layers [ $kg/s * m^3$ ]

$A_o$  ... open flow cross – sectional area [ $m^2$ ]

$C$  ... volumetric concentration, dimensionless

$x$  ... distance along horizontal well [m]

$u$  ... velocity [m/s]

$\rho$  ... density [ $kg/m^3$ ]

$$\begin{aligned} \frac{\partial}{\partial t}(A_o C \rho u) + \frac{\partial}{\partial x}(A_o C \rho u^2) \\ = -C \frac{\partial(A_o p)}{\partial x} - A_o \beta_v (u_l - u_s) \\ - \frac{1}{2} C f \rho u^2 S_o \end{aligned} \quad (3)$$

$f$  ... friction coefficient, dimensionless

$p$  ... pressure in the wellbore [Pa]

$\beta_v$  ... coefficient for drag force [ $kg/(s * m^2)$ ]

$u_l$  ... velocity of liquid [m/s]

$u_s$  ... velocity of solid [m/s]

$S_o$  ... open flow wetted perimeter [m]

$$v_{sl} = \frac{138 (\rho_s - \rho_f) d_s^2}{\mu} \quad (4)$$

$v_{sl}$  ... slip velocity of particle [ft/s]

$\rho_s$  ... density of solid [lbm/gal]

$\rho_f$  ... density of fluid [lbm/gal]

$d_s$  ... diameter of particle [in]

$\mu$  ... fluid viscosity [cp]

Considerable efforts have been made on experimental analysis with help of full-scale flow loops to testify the outcomes of the various models and correlations to evaluate the influence of changing parameters on cutting transport and hole cleaning efficiency.

The earliest studies on cutting transport included the settling of particles in a stagnant drilling fluid, based on Stokes law [11]. Even nowadays the most common and widely spread methods to estimate hole cleaning and predict necessary annular mud velocities are based on, or at least implement, the use of the solids slip velocities in a dynamic fluid [13]. According to Bourgoyne *et al.* (1986) the correlations provided by Walker and Mayes, Chien and Moore gained the highest acceptance, although these correlations did not provide extremely accurate results for determining the particles slip velocity. Nevertheless they deliver valuable information on selecting proper pump operations and drilling fluid properties. The development of these correlations involved trial and error procedures and it was found that Moore's correlation was the most accurate [29].

Moore's correlation provides three different equations for determining the particles slip velocity, depending on whether the flow pattern around the particle is laminar, transient or turbulent. Therefore the first step is to assume a flow pattern and calculate the apparent viscosity  $\mu_a$  of the drilling fluid in centipoise, using equation (5). Depending on the determined flow regime, the slip velocity of the cuttings is determined with the respective equation below. The determined slip velocity and apparent viscosity is then used to evaluate the particles Reynolds number according to equation (6).

$$\mu_a = \frac{K}{144} * \left( \frac{d_2 - d_1}{v_a} \right)^{1-n} * \left( \frac{2 + \frac{1}{n}}{0,0208} \right)^n \quad (5)$$

The consistency index K and the flow index n are calculated using equation (29) and (30).

$$N_{Re} = \frac{928 * \rho_f * v_{sl} * d_s}{\mu_a} \quad (6)$$

If the Reynolds number determined in this way is above 300, the flow is considered to be turbulent and the use of equation (7) is validated.

$$v_{sl} = 1,54 * \sqrt{d_s * \frac{(\rho_s - \rho_f)}{\rho_f}} \quad (7)$$

Otherwise equation (8) is used and the same procedure is repeated.

$$v_{sl} = 82,87 * \frac{d_s^2}{\mu_a} * (\rho_s - \rho_f) \quad (8)$$

If the determined Reynolds number is 3 or lower, the flow pattern is considered to be laminar and equation (8) is validated. If none of the former used equations have been confirmed, the flow pattern is considered to be transient and equation (9) is validated.

$$v_{sl} = \frac{2,90 * d_s * (\rho_s - \rho_f)^{0,667}}{\rho_f^{0,333} * \mu_a^{0,333}} \quad (9)$$

The correlation provided by Chien also contains the computation of an apparent viscosity, using equation (10), except for suspensions of bentonite and water. For them it is recommended to use the plastic viscosity instead of an apparent viscosity.

$$\mu_a = \mu_p + 5 * \frac{\tau_y * d_s}{v_a} \quad (10)$$

The procedure is similar to Moore's correlation. First step is to assume a flow pattern to calculate an apparent or a plastic viscosity and to compute the slip velocity of the particle using either equation (11) or (12). Equation (6) is then used for validation of the assumed flow pattern. If the assumed flow pattern cannot be validated, the alternative slip velocity equation has to be chosen. If the particle Reynolds number is above 100 equation (11) is recommended, otherwise if it is below, equation (12) is valid [12].

$$v_{sl} = 1,72 * \sqrt{d_s \frac{(\rho_s - \rho_f)}{\rho_f}} \quad (11)$$

$$v_{sl} = 0,0075 * \left( \frac{\mu_a}{\rho_f * d_s} \right) * \dots \quad (12)$$

$$\dots * \left[ \sqrt{\frac{36800 * d_s}{\left( \frac{\mu_a}{\rho_f * d_s} \right)^2} * \left( \frac{\rho_s - \rho_f}{\rho_f} \right) + 1} - 1 \right]$$

Similar to the correlations provided by Moore and Chien, the Walker and Mayes correlation includes the computation of an apparent viscosity using equation (13), for determination of the particle Reynolds number with equation (6).

$$\mu_a = 479 * \frac{\tau_s}{\gamma_s} \quad (13)$$

$\tau_s$  ... shear stress [lbm/100 ft<sup>2</sup>]

$\gamma_s$  ... shear rate [RPM]

They worked out a formula (14) for determining the shear stress due to the particle slipping through the fluid, where h is the thickness of the particle in inch.

$$\tau_s = 7.9 * \sqrt{h * (\rho_s - \rho_f)} \quad (14)$$

The corresponding shear rate is then determined using a plot of shear stress vs. shear rate obtained by a standard rotational viscometer. Where the dial reading of the shear stress is multiplied by 1,066 and the shear rate is multiplied by 1,703.

For the determination of the slip velocity the first step is to assume a flow pattern, calculate the apparent viscosity and then choose either equation (15) or (16). Use the derived slip velocity and the apparent viscosity values for determining the particles Reynolds number. For particle Reynolds numbers greater than 100, the flow is considered to be turbulent and equation (15) is recommended. Is the particle Reynolds number below 100, equation (16) is valid [12].

$$v_{sl} = 2,19 * \sqrt{h * \frac{(\rho_s - \rho_f)}{\rho_f}} \quad (15)$$

$$v_{sl} = 0,0203 * \tau_s * \sqrt{\frac{d_s * \gamma_s}{\sqrt{\rho_f}}} \quad (16)$$

After carrying out an extensive experimental study on cutting transport in an 5 inch full-scale flow loop, Larsen et al. (1997) developed a model for proper hydraulics selection to provide sufficient hole cleaning for hole inclinations between 55 and 90 degrees. The experimental study was focused on determining the necessary annular velocity to prevent cuttings from accumulating and depositing on the lower side of the annulus in the wellbore. Based on the experimental outcomes an empirical model was developed to estimate the minimum fluid velocity for suspension flow, the average cuttings travel velocity and the solids concentration in the annular area for velocities below the minimum transport velocity. Furthermore the effects of cuttings size, hole inclination, mud rheology, mud density, drill pipe eccentricity and rate of penetration have been



investigated. Cuttings injection rates were chosen to be 10, 20 and 30 lbm/min, representing an ROP of 27, 54 and 81 feet per hour in a 5 inch hole. An equation was developed for determining the minimum annular fluid velocity, based on the cuttings slip velocity and the velocity at which new cuttings were generated [13].

Ozbayoglu *et al.* (2002) used experimental data, which was received from several conducted cutting transport tests to develop two different models. The experiments were performed at Tulsa University's *Low Pressure Ambient Temperature* (LPAT) cutting transport apparatus. It consists of a test section which is around 100 feet long and has an 8 inch inside diameter transparent outer pipe, with a wall thickness of 1/2 inch. The simulated drill pipe consists of aluminum alloy with an outside diameter of 4,5 inch. Additionally it consists of a 650 gallons injection tank with a rotating auger system for cuttings injection, a shale shaker for removing the cuttings from the drilling fluid which are then collected in a collection tank. The inclinations can be varied from 0 to 90 degrees from vertical. For circulating the drilling fluid a 75 horsepower centrifugal mud pump is used and for air supply a compressor with a working capacity of 0 to 125 psi was chosen. The flow rates of gas and liquid are measured using a Micro-Motion™ mass flow meter. For recording, measuring and controlling the flow rate, inclination, drill pipe rotation and pressure and temperature the LabView™ data acquisition system is used [20].

The result of the first model is an equation with five dimensionless groups of independent drilling variables as inclination angle ( $\pi_1 = \alpha$ ), the feed cuttings concentration ( $\pi_2 = C_c$ , where  $C_c$  is volume of cuttings divided by the volume of the annulus), the fluid density and apparent fluid viscosity ( $\pi_3 = \rho v D / \mu = N_{Re}$ , where  $D$  is the diameter of the flow area and  $v$  the velocity), the total flow rate over the wellbore area ( $\pi_4 = g D / v^2$ ), and the dimensions of the drill pipe and wellbore ( $\pi_5 = A_{bed} / A_w$ ). In order to develop the dimensionless groups the Buckingham- $\pi$  Theorem was used. The equation calculates cutting bed heights for all tested fluids with errors less than 15%. The disadvantage of this model is that different correlations are needed for changing flow regimes, therefore a different correlation is needed for laminar flow regime than from one for turbulent. The second model is called *Artificial Neural Network* (ANN) program, which predicts

bed heights with less than 10% error, by using dimensionless variables like Reynolds Number, Froude Number and cutting concentration at the bit as input variables for the network. The output variable was the cutting bed area. The network recognizes already known patterns and similar patterns, but it has not the ability to recognize new patterns. The advantage of ANN is that the input-output relationship is learned from real data, in contrast to mathematical models which are dependent on assumptions. The main disadvantage is its poor extrapolation capability [20].

Malekzadeh *et al.* (2011) developed a new approach for prediction and calculation of the optimum flow rate for cuttings removal in order to achieve optimized hole cleaning for inclinations from 0 to 90 degrees. Two computer programs were written in MATLAB and combined with each other. The first program combines Larsen's model and Moore's slip velocity correlation together. Larsen's model is used to calculate the minimum flow rate for solids removal from 55 to 90 degrees, while Moore's model is used to calculate the solids slip velocity in vertical wells. The second computer program was developed to predict the optimum flow rate for various drilling fluid rheological properties [15].

### 3 EXPERIMENTAL SETUP

In the following section the overall experimental setup is described which is necessary to realize the experiments, proposed in Chapter 4. The experiments are designed to deliver meaningful values to estimate transport and accumulation properties of solid particles in the annular region of a wellbore. The comparison of these values makes it possible to evaluate the impact of the cuttings shape. Detailed information of the used fluid, the properties of the artificially produced solids, the design of simulation apparatus itself and the necessary equipment is provided.

#### 3.1 Artificial Cuttings

To implement the proposed experiments for investigating the influence of the cutting's shape, it is necessary to use solids with equal physical properties for the differently shaped particles. In the drilling process various shapes of cuttings and cavings are generated, mainly depending on the formation to be drilled, the *Bottom-Hole Assembly* (BHA) used and the drilling process itself. Since the formation and the drilling process vary constantly, in terms of *Weight on Bit* (WOB), *Depth of Cut* (DOC) and *Revolution per Minute* (RPM), the physical properties are strongly different for the generated solids.

In order to investigate one single parameter like the cuttings shape, it is necessary to keep other parameters such as the density, size, surface roughness and the external influences constant. Therefore it is not possible to use real cuttings for investigations on the impact of the solids shape on transport and accumulation characteristics. Furthermore, the size of the cutting transport simulation apparatus, especially the diameter and the annular area of the transparent pipe section, is not in full-scale and hence it is not suitable to use real, full-scale cuttings for investigations. As a consequence, it is necessary to artificially produce solids

with different shapes and sizes, but uniform physical properties. For the design of the artificial solids, the main focus was to ensure equal density, equal surface roughness and the same volumetric amount for the desired shapes, to deliver meaningful and comparable values.

For first experiments on shape investigation two strongly different cutting shapes are chosen. Shape A cuttings are cylindrical solids, similar to cuttings, which are generated by the crushing action of a roller cone bit, with two millimeters in length and diameter. Shape B solids have a nearly plane, ellipsoidal form, which is comparable with cuttings generated by the shearing action of a *Polycrystalline Diamond Compound* (PDC) drill bit.

The density of the artificially produced solids is chosen to be representative for a frequently encountered formation in the drilling process: sandstone. Besides limestone, chalk, dolomite and other types of formations, sandstone is a common reservoir rock, due to its high porosity and permeability and therefore is a frequent target in drilling operations. There exist lots of different types of sandstone formations since sandstone is a sedimentary rock group, consisting of various constituents with different cementation types and grades, changing grain sizes and alternating maturity. Therefore the specific gravities of sandstones vary between around 2 to 3, depending on their composition, maturity, porosity and cementation. The desired specific gravity was on the one hand calculated on the assumption of a pure quartz sandstone with a specific grain gravity of 2,65 with a porosity of 20%, which is filled with water. The calculated mixture density is 2320 kg/m<sup>3</sup>, which on the other hand represents northern "Potsdam" sandstone, as seen in Table 3.1. In order to obtain the specific gravity of 2,32, the synthetic material, which has a specific gravity of 0,94, is mixed with barite powder, which provides a specific gravity of 4,1. The used barite is a natural barium sulfate, which is usually used to increase the weight of drilling fluids, due to its high density. Barite is chemically inert and since it has a red-brown color and is not water-soluble, it is well suited for the planned experiments in the transparent water based drilling fluid.

Stratigraphic unit	Locality	Source of material or depth (feet)	Number of samples	Porosity (percent)			Average bulk density (g/cm <sup>3</sup> )		Reference	Method of porosity determination
				Min-imum	Max-imum	Average	Dry	Water-saturated		
<b>Precambrian</b>										
Goodrich Quartzite..... Nonesuch Shale (calcareous sandstone).	Ishpeming, Mich..... White Pine, Mich.....	Mine..... do.....	..... .....	..... .....	..... .....	..... 5.3	3.24 2.60	..... 2.65	17 16	A-16 A-16
<b>Cambrian</b>										
Antietam Quartzite..... Chickies Quartzite..... "Mt. Simon" sandstone (dolomite). Southern "Potsdam" sandstone.	Marticville, Pa..... Pennsylvania..... Sand Hill well, Wood County, W. Va. Wisconsin.....	Outcrop(?)..... Outcrop..... 13,005-13,165..... Quarry.....	1 5 9 14	..... 3.8 .2 4.8	..... 7.8 2.5 28.3	..... 5.4 .7 11.4	3.05 ..... 2.69 2.30	3.07 ..... 2.70 2.41	17 43 (1) 22	A-16 T-1 A-15 A-1
Northern "Potsdam" sandstone.	do.....	do.....	16	10.4	22.6	19.4	2.13	2.32	22	A-1
Reagan Sandstone..... Sandstone.....	Otis and Penny-Wann fields, Kans. Conley, Great Britain.....	3,449-3,683..... Quarry.....	24 1	5.5 .....	17.8 .....	11.2 6.1	..... 2.45	..... 2.51	123 105	A-9 A-2
<b>Upper Cambrian and Lower Ordovician</b>										
Potsdam and Beekmantown Groups (sandstone).	Ontario, Canada.....	Quarry.....	6	5.0	12.4	8.0	2.44	2.52	112	A-2

Table 3.1: Sandstone Specific Gravity [30]

The compounding process is done with help of an extruder, which allows for mixing together the necessary amount of barite accurately to the liquefied plastic in order to reach the desired density. The total amount of artificial cuttings need to consist of 56,33 % of synthetic material and 43,67 % of barite powder to reach the desired specific gravity of 2,32. The rule of mixtures used for the calculation is visualized in Figure 3.1.

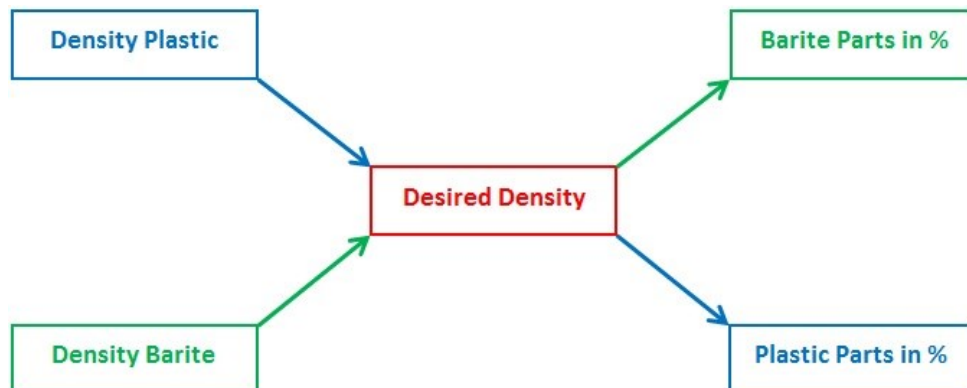


Figure 3.1: Rule of Mixtures

For the experiment on the cuttings transport velocity it is necessary to mix one magnetic particle in the non-magnetic barite cuttings. The production of the magnetic metal cuttings follows the same procedure as the ones made with barite. They have the same size, the same density and the same shape. Therefore the same calculation has to be carried out for these cuttings, but in that case the barite powder is replaced by a stainless ferritic or martensitic steel powder. Steels with higher nickel content develop austenitic structures, which are not magnetic. Therefore austenitic steel powder is unsuitable. The only difference between the barite cuttings and the stainless steel cuttings is the color. The solids made from barite are red-brown, while the ones made from stainless steel are dark grey, which is advantageous for separation.

Since the cutting transport simulation apparatus is not designed in full-scale it is not possible to use real, full-scale cuttings for the designed experiments. Therefore the next necessary step is to downscale the size of the artificially produced solids with the same ratio as derived by the annular area of the simulation apparatus and the annular area of a reference wellbore. The reference wellbore is chosen to be a 21,59 cm (8,5 in) hole with a 17,78 cm (7 in) outside diameter casing or liner. The wall thickness is 1,15 cm (0,453 in) and thereby the inside diameter is 15,47 cm (6,094 in). This provides a cross-sectional annular area of 125,80 square cm (19,5 square in), while the flow loop has a cross-sectional annular area of 25,93 square cm (4,02 square in).

The downscaling procedure is carried out using the geometric similarity theorem, which is applicable for models that have the same shape as the real application and all corresponding dimensions are equal for the model and the prototype. This relationship can be mathematically expressed with equation (17) [7].

$$\frac{A_m}{A_p} = \frac{L_m^2}{L_p^2} = \text{Ratio value} \quad (17)$$

- $A_m$  ... cross – sectional area of the model [m<sup>2</sup>]
- $A_p$  ... cross – sectional area of the prototype [m<sup>2</sup>]
- $L_m$  ... clearance of the model [m]
- $L_p$  ... clearance of the prototype [m]

The size of the generated cuttings varies strongly depending on the drilling process and the encountered formation.

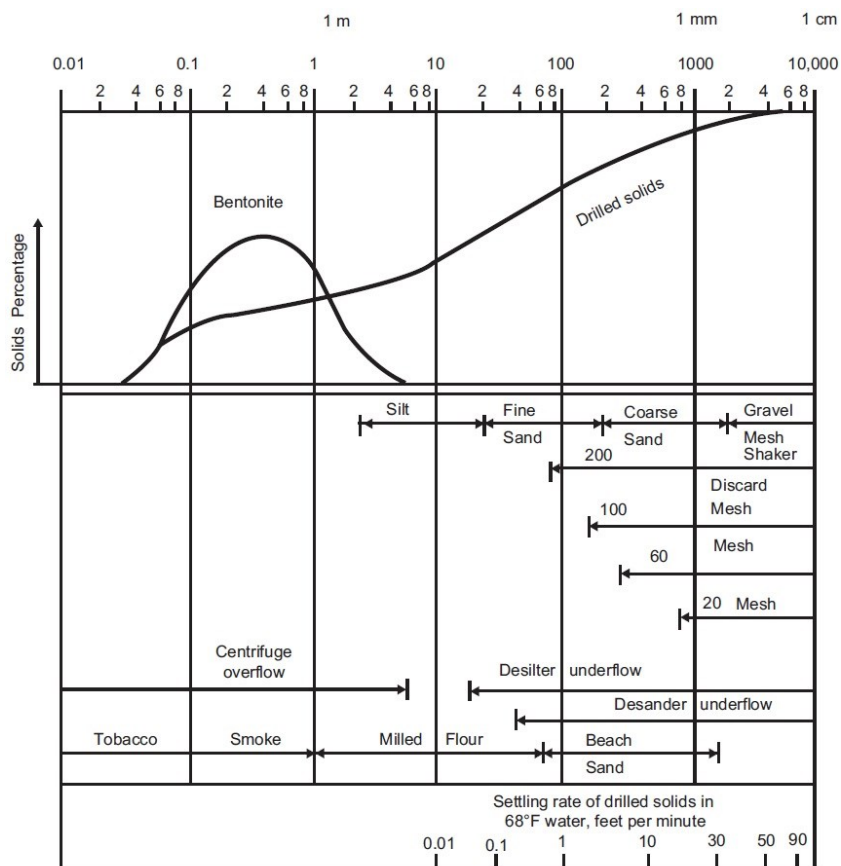


Figure 3.2: Particle Sizes ( [11], p.96)

As a reference value for small sized cuttings, a particle diameter of 10 mm is chosen, according to Figure 3.2. Using the down-scale factor of 0,21, determined

with equation (17), a size of 2 mm is defined for the artificially produced solids. For further investigations additional sizes of 5 and 8 mm are planned, as representatives for medium and big sized cuttings, generated during the drilling process. The upper limiting factor is the diameter of the inner pipe in the measuring unit of the coriolis flow meter, which is 10 mm.

According to Sifferman and Becker (1992) solids concentration between 1 to 4 percent of the fluid volume have only negligible effect on the minimum annular velocity, due to little particle-particle interactions [18]. Therefore the cuttings concentration for the experiments should be chosen to be above 10 volume percent to provide significant interaction between the particles [11].

## **3.2 Fluid Properties**

The drilling fluid and its flow rate is one of the major parameters affecting cuttings transportation and hole cleaning efficiency. In general the fluids found in drilling operations behave very diversely in the circulation systems, on the one hand because of their different rheology and their variable resistance to flow and on the other hand because of changing flow regimes, due to varying velocities.

Near the wall of the conduit the resistance to flow is caused by the friction force acting between the wall on the fluid, which acts in opposite direction of flow and slows down the velocity of the fluid. In the same way the fluid particle, which is slowed down by the friction of the wall, fluid particles further away from the wall of the conduit are slowed down due to the friction forces among the particles themselves and because of the residual influence of the wall roughness. However that influence gradually decreases with increasing distance to the wall. For this reason the velocity of the fluid is highest in the middle of the annular area. The flow resistance or friction forces depend on the fluid properties and the velocities of the fluid particles. Basically the fluids rheology is the study of its resistance to flow and it is described in terms of shear rate and shear stress. With increasing shear rate, shear stress, which is the friction between the fluid particles, is



increased and is measured in terms of shear-force per unit area of shearing layer. The typically encountered fluids in the industry can be classified into five different rheological models, according to their flow behaviour in terms of shear stress provoked by a certain shear rate, seen in Figure 3.5 [8].

The mainly encountered flow regimes in the drilling industry are laminar flow, turbulent flow and, in between, transitional flow. Significant for laminar flow is that the streamlines of the moving fluid are a series of parallel, uniform layers, as illustrated in the picture on the left side in Figure 3.3. On the right hand side streamlines of turbulent flow are visualized with help of a dye tracer [11].

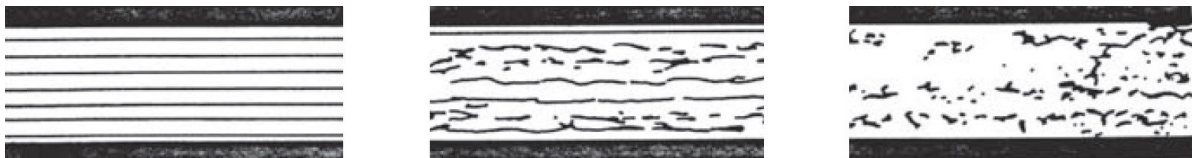


**Figure 3.3: Visualization of Flow Regime with Dye Tracers ( [11], p.246)**

In between there is a transitional flow regime. For very low shear rates, when the drilling fluid has build-up gel strength, additionally plug flow is present. This means the velocity of the fluid in the center of the pipe is the same as on the sides. Usually laminar flow is preferred to transport the cuttings in the annular section to prevent erosion of the *Drill Pipe* (DP) and casing and to minimize friction pressure losses. In terms of wellbore cleaning and cuttings removal however, turbulent flow would be most desirable [11].

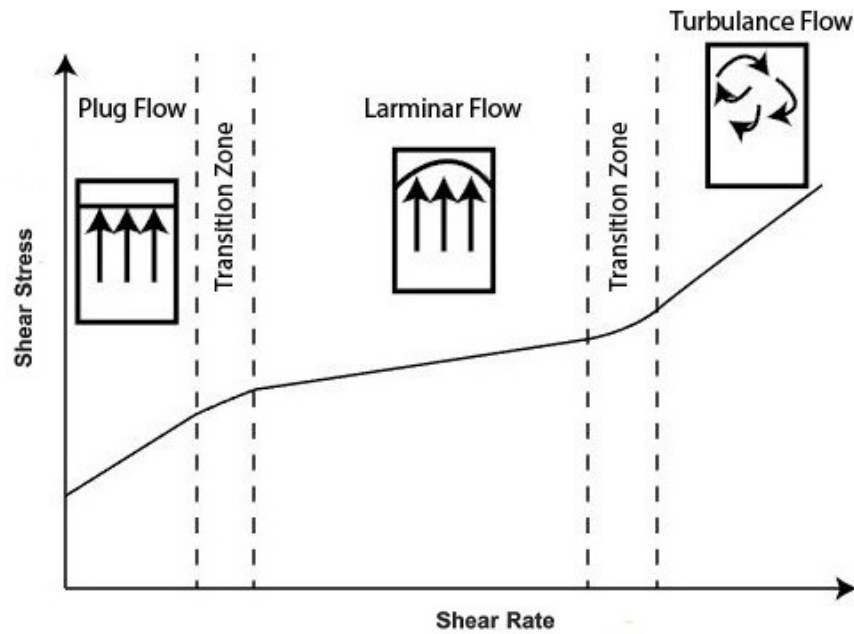


Figure 3.4: Flow Regime Dependence on Shear Rate [31]

A common method to determine the flow regime is to calculate the fluid's Reynolds number. The Reynolds number is a dimensionless coefficient, which describes the ratio between the inertial force and the viscosity force of a fluid in motion. For Newtonian fluids Reynolds numbers below 2100 indicate a laminar flow regime, above 4000 the flow regime is considered to be turbulent and in-between it is considered to be transitional [8]. Usually after every change of the annular cross-sectional area, the flow regime changes to turbulent. As a rule of thumb it takes a length of 20 times the *Inside Diameter* (ID) of the outer pipe to reach laminar flow again.

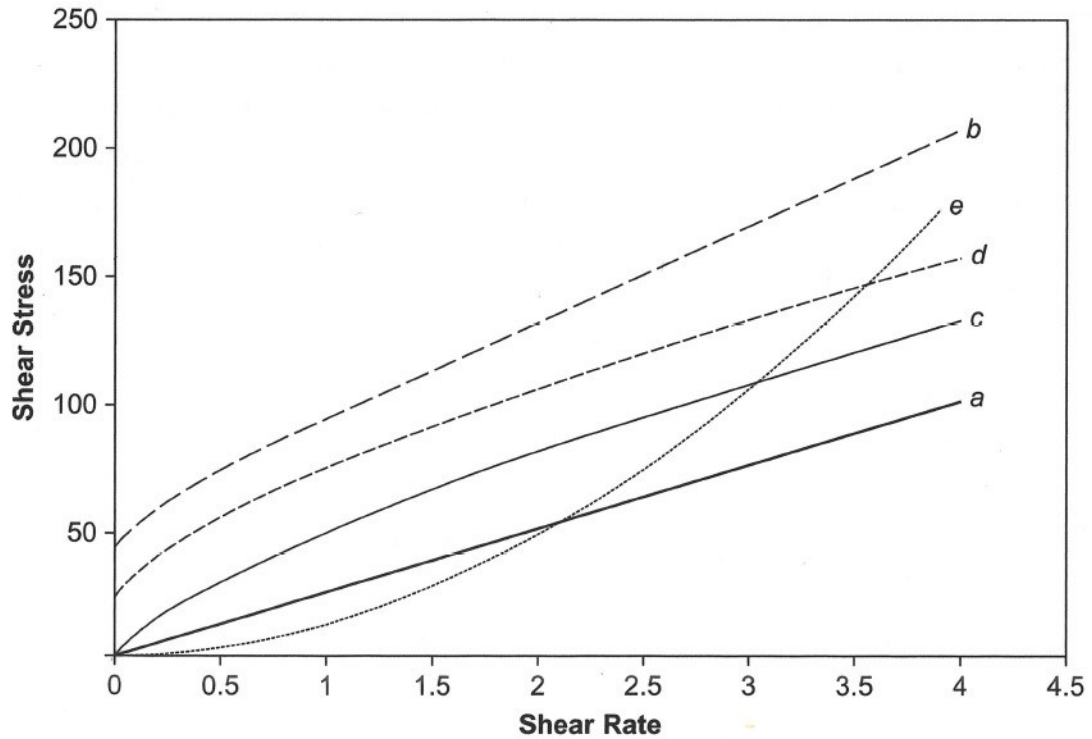


Figure 3.5: Rheological Fluid Models ( [8], p.20)

Curve “a” in Figure 3.5, describes the flow behaviour of typical Newtonian fluids, such as water and mineral oil. For this type of fluid the shear stress increases linearly with the shear rate under laminar flow conditions. The flow behaviour of a Newtonian fluid model can be expressed by equation (18) and the viscosity is calculated by using equation (19).

$$\tau = \mu * \gamma \quad (18)$$

$\tau$  ... shear stress [lbf/100 ft<sup>2</sup> or Pa]  
 $\mu$  ... viscosity [cp or Pa s]  
 $\gamma$  ... shear rate [s<sup>-1</sup>]

$$\mu = \frac{300}{N} * \theta_N \quad (19)$$

$N$  ... rotary speed of viscometer [RPM]

$\theta_N$  ... dial reading of viscometer at rotary speed  $N$  [lbf/100 ft<sup>2</sup> or Pa]

To calculate the Reynolds number of a Newtonian fluid in the annular section of a pipe, equation (20) is used. The constant 757 is valid for U.S. field units and has to be exchanged by 0,816 for *Système International* (SI) units. It is a correction factor to represent the annular cross-sectional area as a diameter value.

$$N_{Re} = 757 * \frac{\rho_f * v * (d_2 - d_1)}{\mu} \quad (20)$$

$d_2$  ... inside diameter of outer pipe [inch or m]

$d_1$  ... outside diameter of inner pipe [inch or m]

$\rho_f$  ... density of fluid [ppg or kg/m<sup>3</sup>]

$v$  ... average flow velocity [ft/s or m/s]

The average flow velocity can be calculated by using equation (21) or (26).

$$v = \frac{Q}{A} \quad (21)$$

$Q$  ... flow rate [gpm or m<sup>3</sup>/s]

$A$  ... annular cross – sectional area [ft<sup>2</sup> or m<sup>2</sup>]

Curve “b” also shows a linear relationship between shear rate and shear stress, except for the low-shear-rate region and describes the flow behaviour of a plastic fluid, or Bingham plastic fluid. In contrast to the Newtonian fluid the shear stress value for a shear rate of zero is not zero. The value at zero shear rate is called “gel

strength” and describes the initial force which is necessary to mobilise the fluid. By adding claylike particles to a Newtonian fluid, its flow behaviour changes to that of a plastic fluid.

The Bingham plastic fluid model can be described by equation (22), where the plastic viscosity is calculated by using equation (23) and the *Yield Point* (YP) is determined with equation (24).

$$\tau = \tau_y + \mu_p * \gamma \quad (22)$$

$\mu_p$  ... *plastic viscosity (PV) [cp or Pa s]*  
 $\tau_y$  ... *yield point (YP) [lbf/100 ft<sup>2</sup> or Pa]*

$$\mu_p = \frac{300}{N_2 - N_1} * (\theta_{N_2} - \theta_{N_1}) \quad (23)$$

$\theta_{N_1}$  ... *dial reading of viscometer at rotary speed  $N_1$  [lbf/100 ft<sup>2</sup> or Pa]*  
 $\theta_{N_2}$  ... *dial reading of viscometer at rotary speed  $N_2$  [lbf/100 ft<sup>2</sup> or Pa]*

$$\tau_y = \theta_{N_1} - \mu_p * \frac{N_1}{300} \quad (24)$$

The apparent viscosity of a fluid for the annular flow region, which follows the Bingham plastic fluid model, is calculated using equation (25). The value 5 is valid for U.S. field units, where the density is given in ppg, the velocity in ft/s, the flow rate in gpm, the diameter in inch and the viscosity in cp. If SI units are used, where the density is given in kg/m<sup>3</sup>, the velocity in m/s, the flow rate in m<sup>3</sup>/s, the diameter in m and the viscosity in Pa s, the constant becomes 0,1253. The average flow velocity in the annulus is derived from equation (26). The constant 2,448 is valid for U.S. field units and has to be exchanged by 0,7854 for SI units.

$$\mu_a = \mu_p + \frac{5 * \tau_y * (d_2 - d_1)}{v} \quad (25)$$

$\mu_a$  ... *apparent viscosity [cp or Pa s]*

$$v = \frac{Q}{2,448 * (d_2^2 - d_1^2)} \quad (26)$$

The Reynolds number is calculated in the same way as for Newtonian fluid, but the apparent viscosity is used. For SI units change the constant 757 to 0,816.

$$N_{Re} = 757 * \frac{\rho * v * (d_2 - d_1)}{\mu_a} \quad (27)$$

Curve “c” describes the flow behaviour of a so called pseudo plastic fluid or Power Law fluid, which is usually typical for polymer solutions. No gel strength build up is observed. The pseudo plastic or Power Law fluid can be described by formula (28), where the dimensionless flow behaviour index n is calculated with equation (29) and the consistency index K is derived by formula (30).

$$\tau = K * \gamma^n \quad (28)$$

$K$  ... *consistency index [cp or Pa s]*  
 $n$  ... *flow behaviour index, dimensionless*

$$n = \frac{\log\left(\frac{\theta_{N_2}}{\theta_{N_1}}\right)}{\log\left(\frac{N_2}{N_1}\right)} \quad (29)$$

If the flow behaviour index “n” fulfils the requirement to be smaller than 1, the model describes a pseudo plastic or Power Law fluid. For  $n = 1$  it describes a Newtonian fluid and for  $n > 1$  the model describes the behaviour of a dilatant fluid.

$$K = \frac{510 * \theta_N}{(1,703 * N)^n} \quad (30)$$

The apparent viscosity for a pseudo plastic or Power Law fluid is calculated using equation (31).

$$\mu_a = \frac{K * (d_2 - d_1)^{1-n}}{144 * v^{(1-n)}} * \left( \frac{2 + \frac{1}{n}}{0,0208} \right)^n \quad (31)$$

The Reynolds number is derived from equation (32) for field units and from equation (33) for SI units.

$$N_{Re} = 109000 * \frac{\rho * v^{2-n}}{K} * \left[ \frac{0,0208 * (d_2 - d_1)}{2 + \frac{1}{n}} \right]^n \quad (32)$$

$$N_{Re} = 909,5 * \frac{\rho * (3,281 * v)^{2-n}}{K} * \dots * \left[ \frac{0,819 * (d_2 - d_1)}{2 + \frac{1}{n}} \right]^n \quad (33)$$

For pseudo plastic or Power Law fluids the criterion of laminar and turbulent flow is determined with help of a critical Reynolds number. Equation (34) defines the upper limit for laminar flow and equation (35) the lower limit for turbulent flow, in between the flow regime is transitional.

$$N_{ReC} = 3470 - 1370 * n \quad (34)$$

$$N_{ReC} = 4270 - 1370 * n \quad (35)$$

Curve “d” characterizes the relationship between shear rate and shear stress of a so-called Herschel-Bulkley fluid. The shear stress increases regressively and the fluid is able to build up a gel strength. The flow behaviour of a fluid following the Herschel-Bulkley model is described by equation (36), where the YP is calculated with equation (37) and the flow behaviour index and the consistency index are derived by using formulas (38) and (39).

$$\tau = \tau_y + K * \gamma^n \quad (36)$$

$$\tau_y = 2 * \theta_3 - \theta_6 \quad (37)$$

$$n = 3,322 * \log\left(\frac{\theta_{600} - \tau_y}{\theta_{300} - \tau_y}\right) \quad (38)$$

$$K = 500 * \frac{(\theta_{300} - \tau_y)}{(511)^n} \quad (39)$$



According to Guo *et al.* (2011) it is valid to treat Herschel-Bulkley fluids as Power Law fluids at high shear rates [8]. For determining the flow regime of a Herschel-Bulkley fluid in the annulus equations (40) - (44) are used in field units. If the calculated Reynolds number is above the critical one, the flow is turbulent, below the critical value the flow is considered to be laminar.

$$N_{Re} = \frac{4 * (2 * n + 1)}{n} * \dots * \left[ \frac{\rho * v^{(2-n)} * \left(\frac{d_2 - d_1}{2}\right)^n}{\tau_y * \left(\frac{d_2 - d_1}{2 * v}\right)^n + K * \left(\frac{2 * (2 * n + 1)}{n * C_a^*}\right)} \right] \quad (40)$$

$$C_a^* = 1 - \left(\frac{1}{n + 1}\right) * \dots * \frac{\tau_y}{\tau_y + K * \left\{ \frac{2 * Q * (2 * n + 1)}{n * \pi * [(d_2/2) - (d_1/2)] * [(d_2/2)^2 - (d_1/2)^2]} \right\}^n} \quad (41)$$

$$N_{ReC} = \left[ \frac{8 * (2 * n + 1)}{n * y} \right]^{\frac{1}{1-z}} \quad (42)$$

$$y = \frac{\log(n) + 3,93}{50} \quad (43)$$

$$z = \frac{1,75 - \log(n)}{7} \quad (44)$$

Curve “e” shows the flow behaviour of a dilatant fluid, which is obtained by adding for example starch to a Newtonian fluid. In contrast to plastic and pseudo plastic fluids, the apparent viscosity increases with increasing shear rate, which is not desirable in the drilling process.

Most drilling fluids are classified as non-Newtonian fluids. This means there is no linear proportionality between shear rate and shear stress. Furthermore they are thixotropic, which means the apparent viscosity decreases, when the shear rate is increased. This is advantageous in drilling operations, because the circulating pressure is reduced and, when circulation stops, the viscosity increases, which lowers the settling velocity of solids in the annulus [8].

For some of the proposed experiments it is required to visually observe the solids behaviour in the transparent annular pipe section of the cutting transport simulation apparatus to determine the desired parameters as the *Critical Annular Flow Velocity (CAFV)*, the *Maximum Annular Flow Velocity (MAFV)*, the *Minimum Transport Rolling Velocity (MTRV)* and the *Minimum Transport Suspension Velocity (MTSV)*. Therefore a diaphanous clarified xanthan gum drilling fluid is used.

According to the manufacturer, clarified xanthan gum is a biological polysaccharide, which is classified to be environmentally harmless. It is a free flowing beige powder, which is 100% water soluble with a specific gravity of 1,5. It is used in the drilling process to produce a low-shear-rate viscosity and high gel strengths, which are very fragile as soon as the circulation is started. Due to these properties and especially because it is transparent, clarified xanthan gum is a superior fluid for cutting transport simulations and for the experiments proposed in Chapter 4 “Experimental Procedures and Objectives” to evaluate the shape influence on solids transportation characteristics. Since clarified xanthan gum generates a low-shear-rate viscosity, this additive provides an improved overall drilling performance. Due to enhanced hydraulics, reduction in torque and drag and reduced formation damage, it thereby contributes to lower the overall drilling costs.

The rheological properties, in terms of shear stress and shear rate, which expresses the fluids resistance to flow, density and gel strength of a 2 g/l, 3 g/l and 4 g/l xanthan-water mixing ratio are provided and tested over a time period of 7 days. The fluid is tested over a period of 7 days to ensure the fluid properties maintain stable while the experiments proposed in chapter 4 are conducted. The fluids properties change over time due to mud conditioning and, without any

further additives, due to degradation. For the rheological property measurements a Chandler Engineering® rotational viscometer and a pressurised TRU-WATE™ fluid density balance are used. The shear stresses of the fluids are determined for the complete set of shear rates and then plotted to identify the fluid's rheology model.

Figure 3.6 shows the provoked shear stresses exerted by the whole set of shear rates, from 1 to 600 rpms of a 2 g/l xanthan-water mud. All fluids are tested 7 days in a row under exact same conditions, at a room temperature of 21 degrees Celsius.

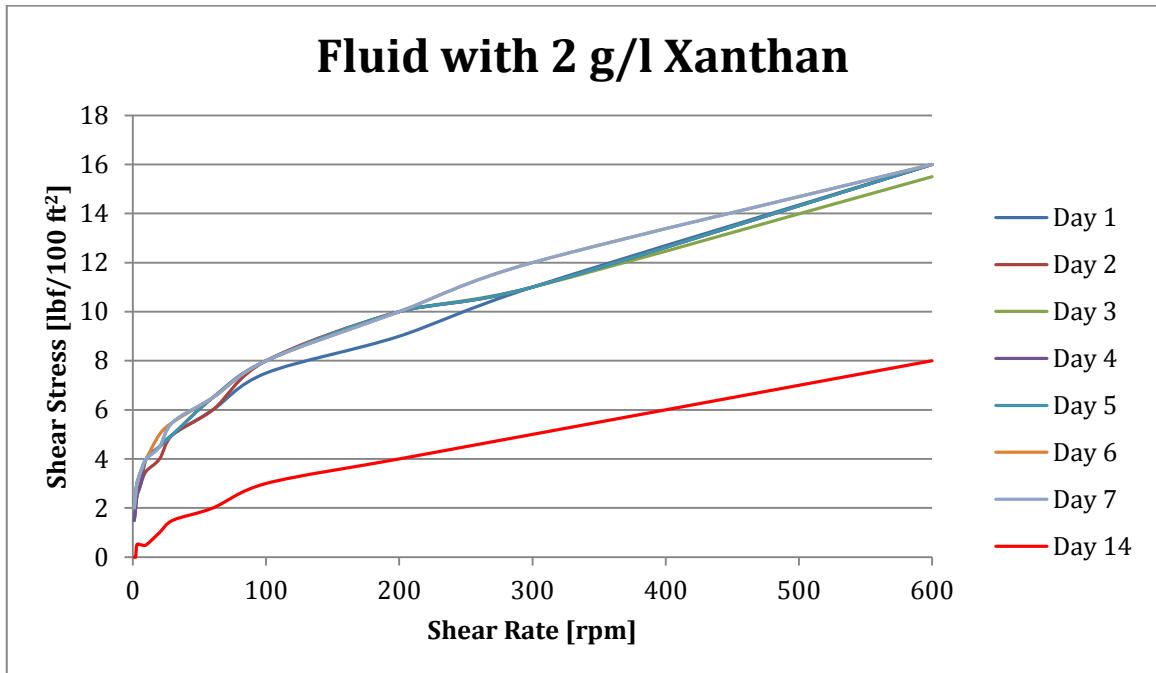


**Figure 3.6: Shear Stress vs. Shear Rate Drilling Fluid 1**

The density of the 2 g/l fluid maintained a value of 971 kg/m<sup>3</sup> and the 10 seconds and 10 minutes gel strength kept constant at 4 and 6 lbs/100 ft<sup>2</sup>. Since xanthan gum is a biological polysaccharide the fluid starts to smell after 14 days and it loses its desired properties. Ten seconds and ten minutes gel strengths both dropped to 1 lbs/100 ft<sup>2</sup> and almost no shear stress was measureable. The red curve indicates the results received after 14 days.

The 3 g/l xanthan-water mud is suggested to be used for the implementation of the experiments, simply because the curves, as seen in Figure 3.7, correspond best with each other, due to minor changes of shear stress values over the tested time period. The density was  $971 \text{ kg/m}^3$  and the 10 seconds and 10 minutes gel strength maintained constant at 8 and 11,5 lbs/100 ft<sup>2</sup>. After 14 days the values decreased to 1,5 and 2 lbs/100 ft<sup>2</sup>.

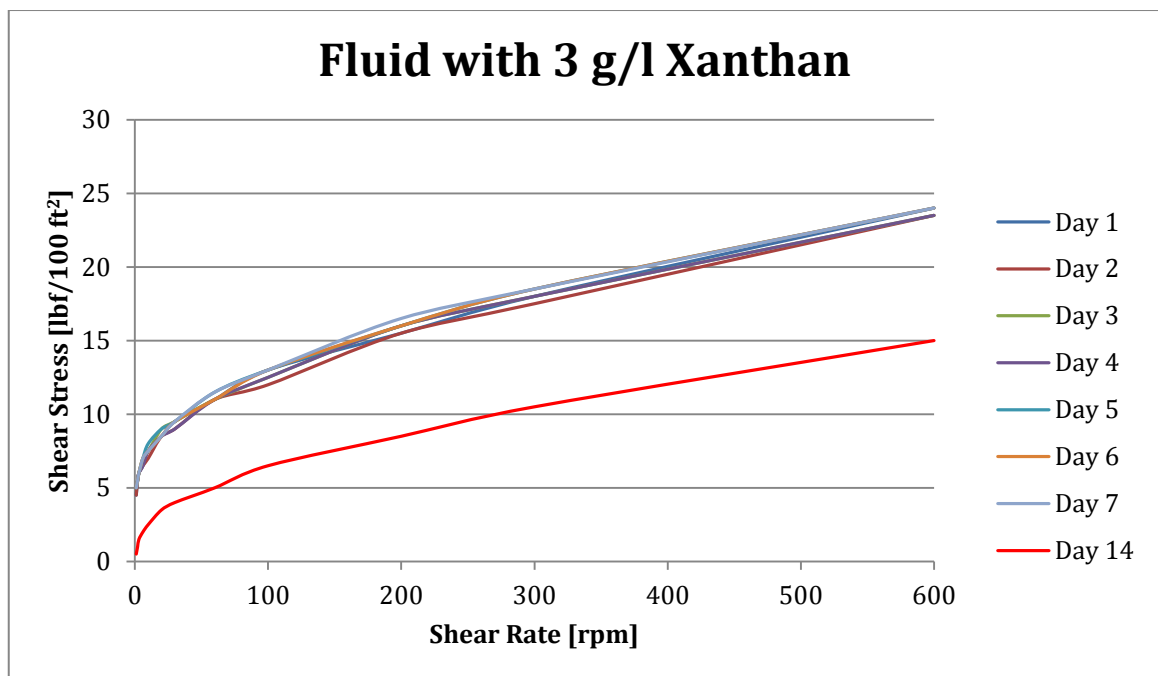


Figure 3.7: Shear Stress vs. Shear Rate Drilling Fluid 2

Figure 3.8 shows the results of the 4 g/l xanthan-water fluid. In this case the measured shear stresses deviate most from each other. The reason might be either insufficient mud conditioning or inaccuracy of measurements, due to excessive viscosity. The 10 seconds and 10 minutes gel strength was 10 and 15 lbs/100 ft<sup>2</sup> respectively and the density was around  $959 \text{ kg/m}^3$ . After 14 days the values decreased to 4 and 4,5 lbs/100 ft<sup>2</sup>.

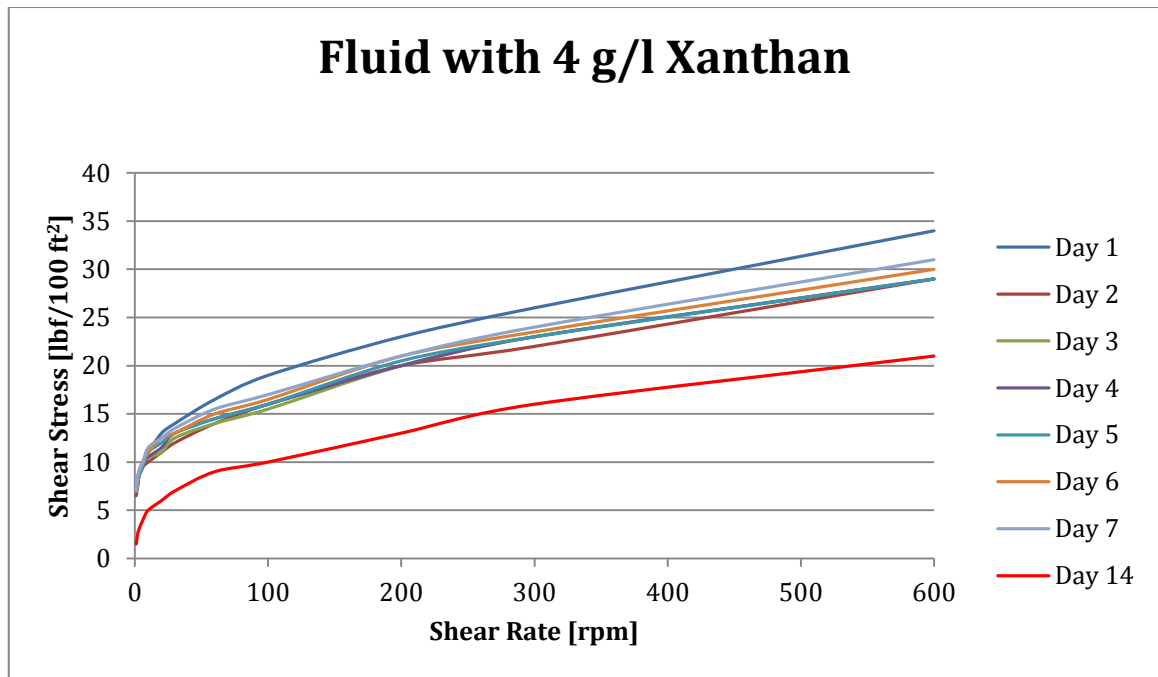


Figure 3.8: Shear Stress vs. Shear Rate Drilling Fluid 3

For this work, where the influence of the solids shape on transport and accumulation characteristics is investigated, it is assumed that the fluid can be rheologically characterised as a Bingham plastic fluid. Since both shapes are investigated and calculated in the same way this assumption seems to be valid.

### 3.3 Solid Transport Apparatus Specification

The following section provides an overview of the design for a cutting transport simulation apparatus, which is necessary for the implementation of the suggested experiments, provided in chapter 4 “Experimental Procedures and Objectives”. Based on that design, investigations of the influence of the cuttings shape on transport and removal efficiency can be conducted. Figure 3.9 provides an overview of the flow schematic and the required equipment.

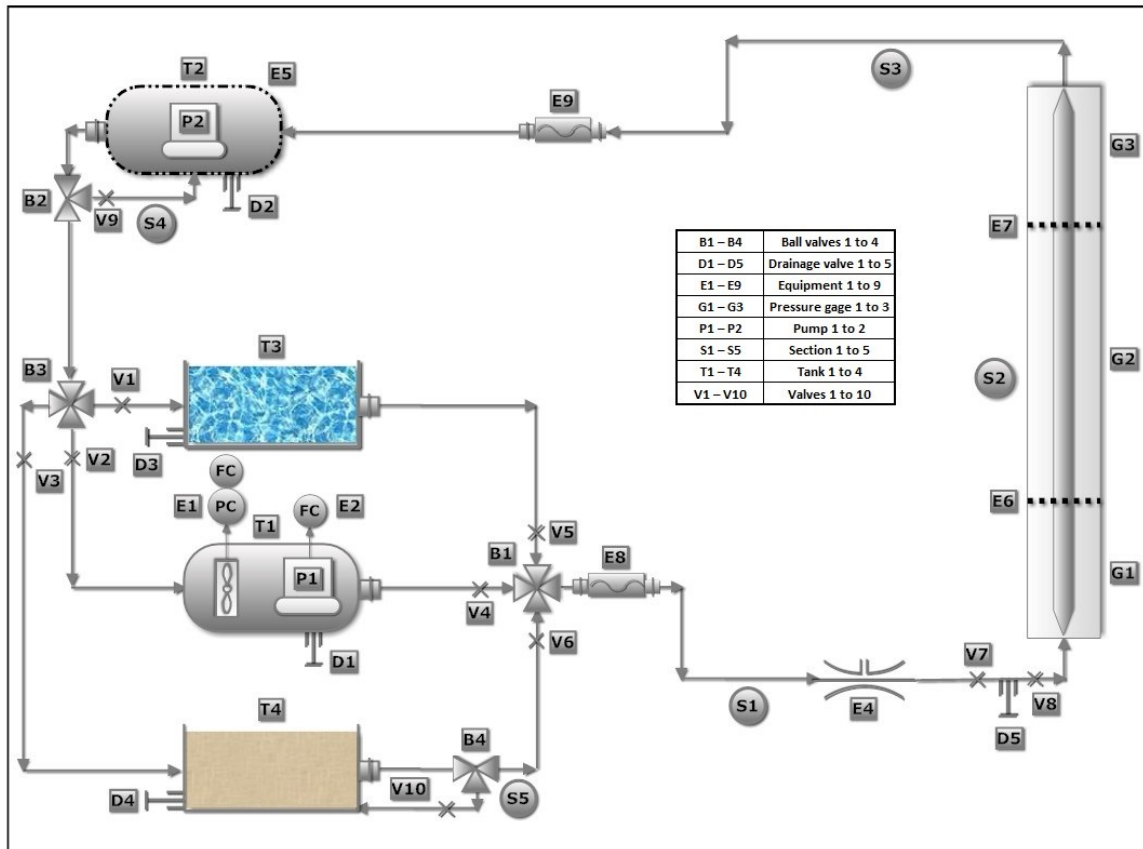


Figure 3.9: Flow Loop Schematic

Basically the suggested design of the cutting transport simulation apparatus, seen in Figure 3.9, consists of four fluid tanks, the surface pipe system, a simulated transparent borehole with a drill pipe inside, two pumps, an agitator, measuring units for mass flow, density, pressure, temperature and current consumption, a venturi pipe with a hopper installation, high-resolution cameras, two metal detectors, pressure sensors and a data acquisition and control unit.

Tank T1 is a round cylindrical 1000 liters stainless steel tank with a convex bottom and a drainage valve D1 installed at the lowest point of the tank. The round shape of the tank is important to avoid deposition of solids in the corners, since this tank is used for most of the experiments for circulating a suspension, consisting of the drilling fluid and the artificial cuttings. Mud pump P1 is positioned inside the tank and it is connected to a frequency converter, termed E2. The frequency converter is necessary to throttle the flow rates for some of the proposed experiments to the

desired minimum. Pump P1 is a portable semi-permanent submersible effluent pump with an engine power of 2,4 kW or 3,2 HP, which is capable of circulating 660 liters per minute with solid particle sizes of 20 mm. The pump consists of stainless steel and cast iron, which makes it suitable for pumping media with medium concentrations of abrasive solids. The maximum discharge head for water is 17 m. The motor is a 3-phase squirrel-cage induction motor with a nominal voltage of 400 V and no starting current, which enables the usage of a frequency converter.

Additionally, to ensure proper conditioning of the previously described drilling fluid and to avoid settling of solids out of the suspension at an early stage, an agitator, termed E1, is installed inside tank T1. A measuring unit for power consumption is connected to the agitator, which provides the possibility for further investigations on density measurements, based on the necessary power consumption of the agitator to stir the fluid. The agitator is operated with an 1,5 kW engine, which delivers 1500 revolutions per minute and can be varied with help of a frequency converter. To implement the frequency converter it is important to use a 3-phase motor with a nominal voltage of 400 V.

Tank T2 is also a round cylindrical 1000 liters stainless steel tank with a convex bottom and a drain valve D2 at the bottom. For circulating the suspension back into tank T1 a second effluent pump P2 is positioned inside the tank. This submersible effluent pump has an engine power of 1,3 kW or 1,7 HP and is capable of circulating 383 liters per minute.

The maximum discharge head is limited to 10 m. To avoid deposition of solids within tank T2, a bypass section labeled S4 is installed to provide a permanent circulation of the suspension within the tank. To regulate the flow rate, that passes through the bypass section, the three way valve B2 and the closing valves V9 is used. A strong coarse sieve with an aluminum frame will be mounted on top of tank T2, which provides the possibility to install a fine stainless steel sieve, termed E5, with a mesh size of 1mm for solids removal. The coarse sieve is necessary to withstand the weight of the sieved cuttings.

Tank T3 and T4 are standardized *Intermediate Bulk Containers* (IBC), both equipped with drainage valves, termed D3 and D4. Tank T3 is used as a water tank to clean the circulation system, while tank T4 contains pure drilling fluid for the *Cutting Bed Erosion Time* (CBET) experiment. To circulate fluid out of tank T3 and T4 pump P1 is used. In the flow line directly after tank T4 another three-way valve B4 and a closing valve V10 is installed. Before pumping fluid from mud tank T4, through the simulated wellbore for research purposes, it is possible to recirculate the drilling fluid for mud conditioning, using the bypass section S5. To rather provide turbulent flow of the fluid inside the tank instead of a rotational laminar movement, it is important to install the reflux valve in the middle of the tank.

All tanks are additionally equipped with an inside scale unit, which is permanently recorded by high-resolution cameras. On the one hand this provides the possibility of a further independent rough measuring unit and on the other hand it is for safety reasons to recognize leakage and to avoid running dry of the pumps.

B1 and B3 are four-way ball valves, while B2 and B4 are three-way ball valves. Both ball valve types are made from stainless steel and have a “T” hole inside, which provides three flow directions. Since the circulated suspension consists of a water-based fluid and solid particles it is advantageous to use stainless steel valves to avoid abrasion and corrosion. To regulate the flow directions, additional closing valves are installed in the flow lines, which are labeled with V1 to V10. The closing valves are ball valves made from stainless steel, which provide two flow directions, due to an “I” hole inside.

The first coriolis mass flow meter is installed in flow section S1, after the four-way ball valve B1. The coriolis mass flow meters are termed E8 and E9 in the figure. These flow meters are capable of measuring the temperature, the mass flow and the density and derived from these values the flow rate and the net flow is determined. Within the coriolis mass flow meters two tubes with an inside diameter of 10 mm are oscillating at a certain frequency, which is calibrated to water. The oscillation frequency is dependent on the density of the pumped fluid. Therefore the frequency change can be used to determine the mass flow. The density measurement has an accuracy of  $\pm 0,0005 \text{ g/cm}^3$ . Since a suspension of



fluid and solids is circulated, the measuring tubes of the flow meters need to be in the upward position to avoid deposition of particles within the measuring tubes. The second coriolis mass flow meter, installed in section S3, is used to determine the point in time when an equilibrium of the cutting bed is reached within the simulated wellbore, using the principles of mass continuity. This feature is necessary for the *Minimum Annular Suspension Velocity* (MASV) experiment.

For further investigations and experiments, based on different cutting concentrations, due to changing ROP's, a venturi pipe with a hopper installation, termed E4, is installed directly before the inlet of the transparent pipe section. The working principle of this eductor pump is based on Bernoulli's principle, which states that an increase in velocity causes a decrease in pressure. The velocity is increased due to a small diameter nozzle inside the venturi pipe. Therefore the operating conditions, especially the flow rates and velocities need to be exactly considered, before determining the type and the size of the eductor pump. Especially to create a sufficient vacuum to suck in the artificial cuttings, the diameter of the jet nozzle within the venturi pipe is important and strongly dependent on the exerted flow rate. For the proposed design of the cutting transport simulation apparatus, the inlet and outlet diameter of the venturi pipe needs to be 50,8 mm (2 in) to fit the surface pipe connections, since the surface pipes have an inside diameter of 50,8 mm and a wall thickness of 3,5 mm (0,14 in). As a reference point, the diameter of the jet nozzle inside the venturi pipe should be around 15,2 mm (0,6 in), but for a more accurate determination it is necessary to determine the necessary flow rates first to sufficiently transport the cuttings and then use Bernoulli's equation to calculate the necessary velocity increase to cause the pressure drop inside the pipe, using equation (45).

$$P_0 + \rho * g * h_0 + \frac{\rho * v_0^2}{2} = P_1 + \rho * g * h_1 + \frac{\rho * v_1^2}{2} \quad (45)$$

$P_0, P_1$  ... pressure at entrance and middle of venturi pipe [Pa]  
 $v_0, v_1$  ... velocities at entrance and middle of venturi pipe [m/s]  
 $h_0, h_1$  ... geodetic height at entrance and middle of venturi pipe [m]  
 $\rho$  ... density of fluid [kg/m<sup>3</sup>]  
 $g$  ... gravitational acceleration [m/s<sup>2</sup>]

On the one hand the use of a venturi pipe installation allows exact control over and variation of the amount of solids added to the liquid stream and thereby observing the impact of changing ROP's on cutting transportation and accumulation tendencies. The solids injection rate can be linked to the ROP using equation (46).

$$Q_{inj} = ROP * A_w * \left( \frac{1}{3600} \right) \quad (46)$$

$Q_{inj}$  ... injection rate [m<sup>3</sup>/s]  
ROP ... rate of penetration [m/h]  
 $A_w$  ... cross – sectional wellbore area [m<sup>2</sup>]

On the other hand it provides the possibility to inject gas, foam and other additives into the liquid stream. This makes further experiments possible to investigate the impact of gas and aerated drilling fluids on deposited solids. Such fluids are used in underbalanced drilling operations to eliminate formation damage and excessive skin in reservoir sections.

D5 is a drainage valve, which is equipped with two closing valves, termed V7 and V8, to allow proper and easy unloading of fluids, either from the transparent pipe section or the tanks themselves.

Section S2 represents the simulated wellbore. It consists of a transparent outer pipe with an inside diameter of 70 mm and a total length of 2 m. Inside the transparent pipe an exchangeable pipe is mounted, which simulates the drill pipe. It can be replaced by a 40, 50 and 60 mm outside diameter pipe for adjustment of

the cross-sectional area of the annulus. The transparent pipe is equipped with two scale units to estimate the cuttings bed perimeter for cutting bed height calculation. The location of the scale units is illustrated in the figure by dotted lines. For some of the proposed experiments, the section between the scale units is used to identify the particles flow pattern and is thereby recorded with a high-resolution camera. Additionally three pressure sensors (G1, G2 and G3) and two magnetic or metal detectors (E6 and E7) are implemented in this section. The basic principle of metal detectors is a live spool, which creates a magnetic field. These detectors are freely positionable to investigate either the impact of turbulent flow, directly after the inlet of the transparent pipe section, or laminar flow in the middle of Section 2. The detectors are connected with a time recorder, which delivers a time stamp as soon as a magnetic particle is detected. The inclination of the simulated wellbore can be varied from 0 to 90 degrees of inclination and is measured using a digital inclinometer. Also the eccentricity of the simulated drill pipe is modifiable.

The frequency converters, the agitator and both pumps are actuated at the control box. All measured data outputs, including flow rate, mass flow, density, temperature, power consumption, time stamps, pressure readings, inclination and the videotaping are displayed at the control box and saved using a data acquisition unit for later analysis.

## 4 EXPERIMENTAL PROCEDURES AND OBJECTIVES

The following section describes the parameters used to investigate the solid shape influence on transportation and accumulation characteristics. Furthermore it provides a step by step guidance to implement seven developed experiments with the proposed design of the cutting transport simulation apparatus.

### 4.1 General Parameters

The research results published by fellow investigators showed some major parameters for the observation and evaluation of the cutting transport efficiency for vertical, inclined and horizontal wellbore sections. These parameters have to be monitored and controlled to estimate cuttings removal from the bottom of the wellbore and their transportation up to the surface. Malfunctions in removal and transportation of the generated solids cause problems such as reduction in *Rate of Penetration* (ROP), mechanical pipe sticking, increase in torque and drag, which may limit the reach necessary to hit the target, difficulties in casing or liner running jobs, wellbore stability problems, excessive over-pull on trips, lost circulation and an increase of bit wear. In general, besides *Health, Safety and Environmental* (HSE) risks, the overall project costs rise and the profit decreases.

Main parameters used for experimental and empirical determination of hole cleaning and transport efficiency are:

- Total weight of the cuttings in the wellbore
- The height of the solids bed
- Solids concentration in suspension

- *Minimum Transport Rolling Velocity (MTRV)*
- *Minimum Transport Suspension Velocity (MTSV)*
- Slip velocity of particles

The “*Minimum Transport Rolling Velocity*” is the necessary flowing velocity in the annulus to maintain a moving cutting bed rather than a stationary cutting bed. The necessary velocity in the annulus to avoid settling of solids out of the suspension and deposition to cutting beds is called “*Minimum Transport Suspension Velocity*” [32].

In order to evaluate the influence of the particle shape on transportation properties, some of these parameters are suggested for observation and comparison between the two previously mentioned shapes of cuttings. Therefore experiments are suggested to be conducted with help of the proposed design of the cutting transport simulation apparatus and in the laboratory.

The flow loop provides vision on the transport behaviour of the cuttings, which allows the observation of the cutting flow behaviour and the detection of desirable or undesirable modes of transportation. Generally it is desirable if cuttings move upwards the annulus along the wellbore. The differentiation for the experiments between desirable and undesirable modes of transportation is as follows.

**There are four desired flow patterns:**

1. Suspension flow
2. Suspension flow with moving cutting bed
3. Mainly moving cutting bed and partially stationary
4. Laminar flow

**Undesired flow patterns are:**

1. Dune movement
2. Mainly stationary cutting bed and only partially moving
3. Stationary cutting bed

The suggested experiments make it possible to determine the flow rates that provoke certain modes of transportation and which are necessary to erode an already formed cutting bed. The gained flow rates can then be converted into velocities in m/s, representing a minimum or maximum velocity value for a certain flow pattern.

Furthermore the cuttings final transport velocities can be measured, which in turn enables to calculate the cuttings slip velocities. The determined parameters provide meaningful values for comparison between the two artificially produced shapes of solids.

Besides flow rates and velocities, a further parameter which can be investigated is the *Cutting Bed Height (CBH)* in the annular section. The bed height is determined by measurement of the cutting bed perimeter in a test section, after a predefined time of circulation with a chosen velocity. The test section is a 20 cm interval in the middle of the transparent pipe section, visualized by two scale units, termed E6 and E7 in Figure 3.9. The scale unit is used to define the bed perimeter, which can be converted into a cutting bed height. For determination of the flow rates the coriolis mass flow meter E8 is used.

Another investigated parameter is the necessary duration of circulation with a predefined flow rate to erode an already formed cutting bed.

To provide a good comparison of the transport behavior for both shapes, every experiment has to be repeated several times to ensure the obtained values of velocities and bed heights are reproducible and meaningful. The results are then

compared between both shapes for estimation of the shape influence on cutting transport and accumulation behavior.

The magnitude of the velocities exerted in the experiments can be seen in Figure 4.1.

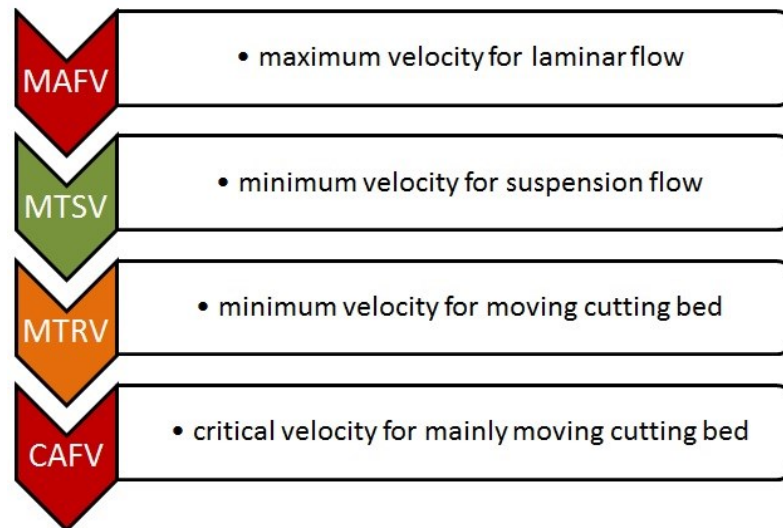


**Figure 4.1: Magnitude of Determined Velocities**

The proposed design of the flow loop and the implemented equipment additionally allows for the investigation of the effects of changing inclinations, different drill pipe eccentricities, various fluid rheology types, the impact of aerated fluids and foams and different ROP's.

The flow chart seen in Figure 4.2 outlines the experiments, the measured values, determined parameters and further parameters which can then be derived consecutively. The boxes shaded in green represent the parameters which are determined in the first place and are necessary for the determination of further parameters which are shaded in red. The boxes shaded in grey contain the developed experiments and the boxes shaded in yellow represent the values which are directly measured during the experiment to enable the determination of the desired parameters.

The developed experiments, the measured parameters and the detailed implementation of the experiments are described in the following section.

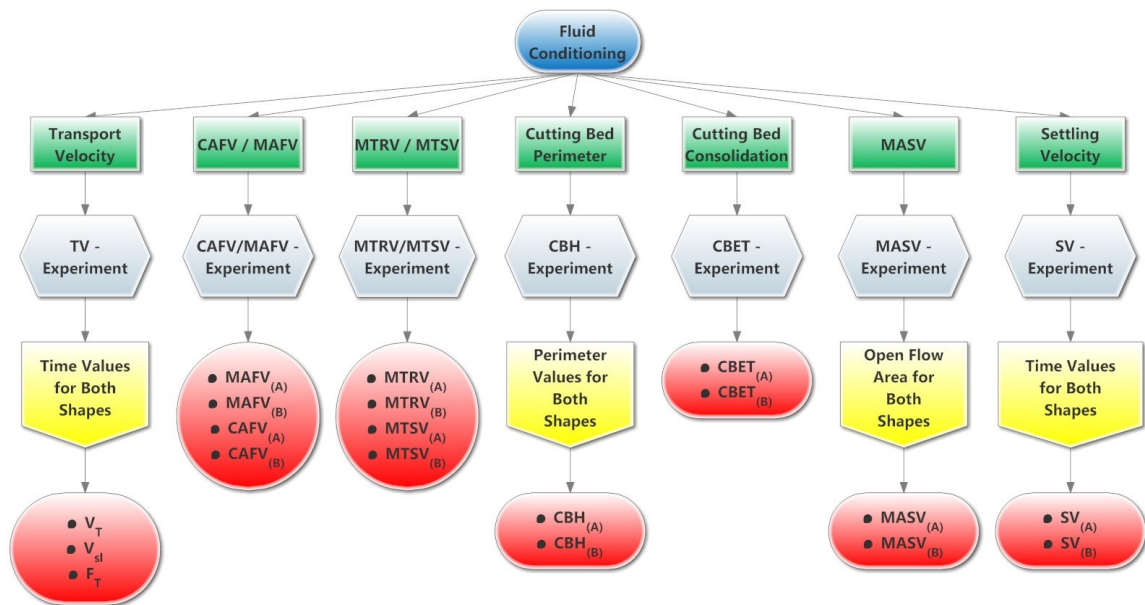


Figure 4.2: Experiment Flow Chart

## 4.2 TV - Experiment

### Transport Velocity – Measured Parameter Definition:

For vertical wellbores the settling velocity of the cuttings is an important parameter to estimate. The settling velocity is the velocity at which solids settle to the bottom of the wellbore due to their gravitational force and it equals the slip velocity between the cuttings and the fluid. The settling velocity of the cuttings does not only have a major impact on vertical, but also on horizontal wellbore sections. The slower the settling velocity, the bigger the horizontal distance the solids travel due to the momentum of fluid before they reach the lower side of the annulus. A proper prediction of cutting settling velocity helps to estimate the cuttings concentration more precisely, which leads to an improved control of the pressure profile in the annulus. Furthermore an accurate prediction of the settling



velocity enables more precise lag time determination and therefore better depth estimation, since the cuttings received on the surface can be correlated to the depth from where they were generated. This helps to get more exact information about lithology, porosity, pore pressure and permeability of the drilled formation [33]. The settling velocity is strongly influenced by drilling fluid rheology, the particle size, density and shape, the resting time of the mud and the annular velocity. The settling velocity of the two different shapes under static conditions is measured in the laboratory.

Therefore a major parameter worth to be investigated to evaluate the influence of the cuttings shape on transport behavior is the cutting slip velocity. Since the slip velocity is a function of densities, diameter and annular fluid velocity, which implements the windage of the solids, it is an excellent parameter to compare the two different shapes of cuttings. The *Transport Velocity - Experiment* provides an accurate experimental determination of the solids transport velocity in the annular section. It includes the consideration of the interaction between the cuttings themselves and the fluid in annular pipe flow. Furthermore the impact of fluid rheology, flow regime, temperature, inclination, drill pipe eccentricity and varying cutting concentrations due to changing ROP's can be observed and determined. A meaningful determination of the cuttings transport velocity enables a direct calculation of the cuttings slip velocity, since the annular flow velocity, which is necessary to know, is a function of the flow rate provided by the pump. The flow rate of the fluid is directly measured with help of a coriolis mass flow meter installed in section S1.

The proposed experiment enables the experimental determination of the cuttings transport velocity  $V_T$  and hence a meaningful estimation of the cuttings slip velocity,  $V_{sl}$ . This allows the comparison of different available slip velocity correlations provided by the literature, mentioned in chapter 2.3. Additionally it provides the possibility to develop a correction factor for the slip velocity correlations. Furthermore, since the particle diameter is a function of the slip velocity equations provided by Chien and Moore, it provides the possibility to generate a new sphericity correction factor.

**Experiment step by step implementation:**

**Step 1:** The first step for the implementation of the *TV - Experiment* is to agitate the drilling fluid with help of the high revolution agitator E1 to provide proper mud conditioning. Different kinds of drilling fluids can be used for this experiment, since no visual observation of the solids behavior is required. While stirring the mud, both pumps are switched off. One has to make sure that two metal detectors are mounted properly and in the right position, which is dependent on the desired flow regime to be observed. This is either at the entrance of the transparent pipe section for turbulent flow observation or in the measuring section in the middle of the pipe to study laminar flow.

**Option 1:**

**Step 2:** After providing enough time for mud conditioning to ensure stable fluid properties, the drilling fluid is pumped from tank T1 into tank T2 with pump P1. Since the four way ball valve B1 provides three flow directions at once, it is necessary to close valves V5 and V6. The mass flow and the density reading of the coriolis mass flow meter E8 is used to determine the volume flow in section S1, using equation (47), which can then be converted into an annular fluid velocity in section S2.

$$\dot{V} = \frac{\dot{m}}{\rho} \quad (47)$$

$\dot{V}$  ... volume flow [ $m^3/s$ ]

$\dot{m}$  ... mass flow [ $kg/s$ ]

$\rho$  ... density of drilling fluid [ $kg/m^3$ ]

The used settings of the pump and the determined volume flow are recorded. Then the fluid is pumped back into tank T1, using pump P2, while the valves V9, V1 and V3 are closed.

**Step 3:** Now the artificial cuttings, which consist of synthetic material and barite, are added to mud tank T1. The suspension is agitated for another 5 minutes to ensure a uniform solids distribution. The previously used settings are used to circulate the suspension of the drilling fluid and solids into tank T2. Again the mass flow and the density reading of the coriolis mass flow meter E8 is used to determine the volume flow in section S1. The volume flow of pure drilling fluid determined in Step 2 is compared with the volume flow of the suspension, determined in Step 3. If both values are equal, possibility 1 is valid to use, which in turn would save time, because it is possible to circulate the suspension instead of filtering the cuttings from the fluid after every single circulation. In case that the volume flow values differ from each other, possibility 2 has to be used.

**Option 2:**

**Step 2:** Install the sieve E5 on tank T2, close the ball valves V5, V6, V9, V1 and V3 and start circulating the drilling fluid into tank T2. Switch on pump P2 to provide permanent circulation of the fluid through the loop system.

**Step 3:** After providing enough time for mud conditioning to ensure stable fluid properties, the artificial cuttings, compound of synthetic material and barite are added to the volume flow using the venturi injector with a hopper E4. The valve position of the hopper can be used to regulate the mass inflow of solids.

**Continue:**

**Step 4:** Depending on which possibility is chosen, one cutting composed of synthetic material and stainless steel is added either to the suspension in tank T1, after the whole pipe system is filled up or to the volume flow using the venturi injector E4. In case that the hopper is used, the stainless steel particle is added after the transparent pipe section S2 is filled with cuttings made of barite to ensure the cutting concentration is high enough to provide particle-particle interaction. Once the stainless steel cutting is added, the flow rate of pump P1 has to be chosen high enough to avoid deposition and accumulation of solids within the pipe system. With help of the metal detectors E6 and E7 the particle with stainless steel will be detected within the barite cuttings of the same shape, size and density. The

time it takes for the metal particle to pass the first and then the second detector is measured and recorded. Since the distance between the detectors is known, the transport velocity of the cutting can be calculated by dividing the travelled distance by the travelling time, shown in equation (48).

$$V_T = \frac{s}{t} \quad (48)$$

*t ... cutting travelling time [s]*  
*s ... distance between detectors [m]*  
*V<sub>T</sub> ... transport velocity of cutting [m/s]*

**Step 5:** The mass flow, recorded with help of the coriolis mass flow meter E8 in the pipe section S1, is then converted into volume flow using equation (47), which can then be converted into an annular fluid velocity present in the transparent pipe section S2, using the equations (49) and (51).

$$Q_1 = Q_2 \quad (49)$$

*Q<sub>1</sub> ... flow rate in section S1 [m<sup>3</sup>/s]*  
*Q<sub>2</sub> ... flow rate in section S2 [m<sup>3</sup>/s]*

Q<sub>1</sub> is the flow rate in pipe section S1, determined with help of the coriolis mass flow meter E8 and Q<sub>2</sub> is the flow rate in the annular area of the transparent pipe section S2. The flow rate is a function of area A and velocity V, shown in equation (51) and the annular cross-sectional area of section S2 is calculated using equation (50).

$$A_2 = \frac{(d_2^2 - d_1^2) * \pi}{4} \quad (50)$$

$A_2$  ... annular cross – sectional area in section S2 [ $m^2$ ]

$d_1$  ... outside diameter of inner pipe [m]

$d_2$  ... inside diameter of outer pipe [m]

$$Q = A * V \quad (51)$$

Therefore combining the above equations (49) and (51) derives the annular fluid velocity in the transparent pipe section S2.

$$V_2 = \frac{Q_1}{A_2} = \frac{A_1 * V_1}{A_2} \quad (52)$$

$A_1$  ... cross – sectional area of section S1 [ $m^2$ ]

$V_1$  ... fluid velocity in section S1 [m/s]

$V_2$  ... annular fluid velocity in section S2 [m/s]

The knowledge of the annular velocity of the drilling fluid and the transport velocity of the solid enables to calculate the slip velocity of the particle using equation (53).

$$V_T = V_2 - V_{sl} \quad (53)$$

$V_{sl}$  ... solid slip velocity [m/s]

**Step 6:** After all variables have been determined, pump P1 is switched off and pump P2 is used to circulate the suspension or drilling fluid back into tank T1. To avoid deposition of solids in tank T2 use the bypass valve B2 to agitate the suspension. When using bypass section S4, the ball valve V9 must be in open position. After circulating the suspension back into tank T1 use drain valve D2 to release the dead volume of tank T2. To ensure the received time values are meaningful and reproducible, repeat step 1 to 6 for further 2 times for cutting shape A.

**Step 7:** After the third round of the experiment for cutting shape A, the solids get removed from the liquid. Therefore the sieve E5 is installed on mud tank T2. Pump P2 is switched on to circulate the suspension back into tank T1. The agitator E1 is switched on and a high flow rate is chosen for pump P1 to whirl up and remove deposited cuttings in the pipe system. The bypass section S4 is opened to provide back circulation and stirring in mud tank T2 to lift deposited cuttings from the bottom and corners. Circulation is continued until no cuttings are collected anymore at the sieve. When no more cuttings are retrieved, switch off pump P1 to fill up mud tank T1 again with drilling fluid. The dead volume in tank T2 is bleed off with help of the drainage valve D2. The sieve is removed, the cuttings are cleaned with clear water and the stainless steel particle is sorted out.

**Step 8:** Repeat step 2 to 7 with cutting shape B.

**Step 9:** After evacuating the remaining drilling fluid from tank T2, pump P1 is switched into tank T3, which is filled with fresh water. The ball valves V4 and V6 are closed, while valve V5 is opened. The water is circulated with pump P1 at high velocity through the transparent pipe section into tank T2. Pump P2 is used to circulate from tank T2 back into tank T3. This allows continuous circulation of fresh water through the pipe systems. During circulation of fresh water the valve B2 is used to clean the bypass section S4. After the loop system is cleaned, the valve V5 is closed and pump P1 is switched off. Pump P2 circulates the remaining water from tank T2 back into tank T3. The remaining water in the pipe system is released using the drainage valve D5. Section S2 is slightly lifted and the ball valve

V7 is closed. The dead volume of water remaining in tank T3 is bleed of using drainage valve D2.

**Values recorded in the TV - Experiment:**

- 3 time values for determination of cutting transport velocity  $V_{T(\text{Shape A})}$ .
- 3 time values for determination of cutting transport velocity  $V_{T(\text{Shape B})}$ .

Besides the determination of the cutting transport velocity and the particle slip velocity, this experiment enables the evaluation of the fluid's transport ratio  $F_T$ . To remove the generated cuttings from the bottom of the wellbore and transport them to the surface, besides other factors, a minimum mud flow rate and thereby a *Minimum Transport Velocity* (MTV) is required. The MTV is the necessary velocity to maintain an upward movement of the generated cuttings and avoid deposition or accumulation of solids in the wellbore. The MTV concept can be used to estimate hole cleaning in horizontal and highly inclined sections. The slip velocity concept in turn can be used to determine the MTV necessary to keep the cuttings moving upward in the annulus and avoid deposition and accumulation in the annular area of the wellbore [15]. Hole cleaning is generally modeled by using the *Cutting Transport Ratio* ( $F_T$ ), which is a good measure of the carrying capacity of a certain drilling fluid [32]. The cutting transport ratio is defined to be the transport velocity ( $V_T$ ) of the solids divided by the annular velocity ( $V_a$ ) of the drilling fluid, which are diverging from each other due to the interfacial slip.

$$F_T = \frac{V_T}{V_a} \quad (54)$$

Combining equations (54) and (1) lead to the relation shown in equation (55).

$$F_T = \frac{V_T}{V_a} = 1 - \frac{V_{sl}}{V_a} \quad (55)$$

The cuttings will travel to the surface if the cutting transport ratio corresponds to a positive value. Assuming a cutting slip velocity of zero, which means the solids travel at the same speed as the fluid does cause a transport ratio of 1, or 100 %. For vertical wellbores the cutting transport ratio should be above 0,5 to ensure efficient hole cleaning. This means the minimum annular fluid velocity needs to be two times the slip velocity of the rock fragments to provide proper solids removal [2].

### 4.3 CAFV/MAFV - Experiment

#### **CAJV/MAJV - Measured Parameter Definition:**

In the *CAJV/MAJV - Experiment* the minimum necessary velocity to achieve a desired flow pattern, as listed in 4.1, is called *Critical Annular Flow Velocity* (CAJV). Below the CAJV solids not only settle out of the liquid phase, they start already depositing on the bottom of the pipe forming a cutting bed, which is partially moving, but mainly a stationary cutting bed, which is, as mentioned before, an unfavourable mode of transportation, since most of the cuttings are not carried from the bottom of the wellbore to the surface. Furthermore the DP gets buried by deposited solids, which would cause problems in the drilling process as excessive torque and drag and increase in stuck pipe tendency.

The upper range of velocities above which an undesired flow pattern in regard to turbulent flow is observed, is called *Maximum Annular Flow Velocity* (MAJV). Turbulent flow is most preferable from the standpoint of cuttings removal and hole cleaning, but causes an increase in pressure losses due to friction in the annular area. A large amount of power is consumed during drilling operations for circulation of the drilling fluid. Therefore it is preferable to go for a minimum,



power saving annular velocity, sufficient for cuttings removal and transportation [34]. The spent power can then be used to increase the *Measured Depth* (MD).

In the *CAFV/MAFV - Experiment* the absolute lower and upper limit of velocities necessary to obtain a desired mode of transportation is defined. It delivers a range of values within efficient hole cleaning is guaranteed. The velocity range varies from close to turbulent flow down to the occurrence of a mainly stationary bed.

Figure 4.3 shows the flow pattern caused by the CAFV, a partially moving but mainly stationary cutting bed.



**Figure 4.3: Mainly Stationary Bed and Partially Moving**

The flow pattern caused by the MAFV is shown in Figure 4.4. All solids maintain in suspension since the flow regime is close to turbulent and no formation of cutting beds can be observed.



**Figure 4.4: Suspension Flow**

**Experiment step by step implementation:**

**Step 1:** To provide proper mud conditioning, the first step of the implementation of the *CAFV/MAFV - Experiment* is to agitate the transparent drilling fluid at high velocity with help of the high revolution agitator E1. In this stage both mud pumps are switched off. The transparent pipe section is completely horizontal. Tank T4 is not needed for this experiment. Make sure the ball valves V7 and V8 are open.

**Step 2:** Then the artificial cuttings are added to the drilling fluid in mud tank T1, starting with shape A. The slurry is circulated within the tank for another 5 minutes to ensure proper stirring and a uniform distribution of solids.

**Step 3:** Next step is to switch on pump P1 and circulate the suspension at high velocity through the annular section into mud tank number T2. Since the four way ball valve B1 provides three flow directions at once, it is necessary to close valves V5 and V6. The cuttings transportation behavior is observed in the measuring section of the transparent pipe. Near the entrance and exit of the transparent pipe, turbulent flow is present due to the diameter change and the presence of the simulated drill pipe. Therefore the observation section is limited to 20 cm in the middle of the transparent pipe section S2. Since the flow rate is high, no solids are depositing or accumulating, but turbulent flow can be observed, hence an undesired flow pattern is present. The flow rate is reduced with help of the flow controller until laminar flow is reached. As soon as laminar flow is established the flow rate is recorded.

**Step 4:** The recorded flow rate of the pump P1, which is measured in pipe section S1, is then converted into an annular velocity term, which represents the MAFV value, with help of equation (49), (51) and (52). This value represents the upper limit of the desired velocity range to achieve a desired flow pattern.

**Step 5:** (Optional) In case that not enough fluid is left in mud tank T1 to complete the experiment due to the high flow rate applied, switch on pump P2 to continuously circulate back from mud tank T2 into mud tank T1. Since in this stage of the experiment no cuttings have deposited or accumulated due to the high

circulation velocity and the additional use of the agitator in the tank T1, the solids distribution in the drilling fluid remains constant.

**Step 6:** After the determination of the MAFV value, the flow rate is reduced further till such time when cuttings start to settle out of the fluid and deposit on the lower side of the annulus, forming a moving cutting bed on the bottom of the pipe in section S2. Continue circulation with the chosen flow rate for a couple of minutes and check if the formation of a stationary cutting bed can be observed. If a mainly stationary and partially moving cutting bed is observed, record the flow rate of pump P1. Otherwise decrease the flow rate further, step by step, until a stationary cutting bed is predominant. Again, in case that not enough fluid is left in mud tank T1 to complete the experiment, switch on pump P2 to continuously circulate back from mud tank T2 into mud tank T1.

**Step 7:** The flow rate determined in step 6, where a mainly stationary cutting bed is formed, is converted again with equations (49), (51) and (52) into an annular velocity. This value represents the CAFV value. At this point the cutting bed is mainly stationary and partially moving, representing an undesired flow pattern. Above this critical value a desirable flow pattern is observed.

**Step 8:** Last procedure is to increase the flow rate of pump P1 to its maximum to bring the deposited cuttings back into suspension and erode the formed cutting beds. At the same time switch on pump P2 and circulate the suspension back to mud tank T1. Using both pumps simultaneously allows permanent circulation through the pipe system. To avoid deposition of solids in tank T2 the bypass section S4 is used.

**Step 9:** To ensure the received values are meaningful and reproducible, repeat step 1 to 8 further two times for shape A.

**Step 10:** After the last round the solids with shape A get removed from the liquid. Therefore a sieve E5 is installed at mud tank T2. Pump P2 is switched on and a high flow rate is chosen for pump P1 to establish turbulent flow to whirl up deposited solids in the pipe system. Use the bypass section S4 to implement a radial velocity in tank T2 to remove cuttings from the bottom and corners.

Continue circulation until no solids are collected anymore at the sieve. When no more cuttings are retrieved, switch off pump P1 to fill up mud tank T1 again with drilling fluid. Remove the sieve, clean the artificial cuttings with water and let them dry.

**Step 11:** Repeat step 2 to 10, with cutting shape B.

**Step 12:** To clean the pipe system evacuate the drilling fluid from tank T2 by switching off pump P1. Pump P2 is used to circulate the remaining drilling fluid back into mud tank T1. The dead volume of tank T2 is released with help of the drain valve D2. The ball valves V6, V4, V3, and V2 are closed, while valve V5, V1 and V9 are opened. Then switch the pump P1 into tank T3, which is filled with fresh water and circulate at high velocity through the pipe system into mud tank T2. Pump P2 is used to circulate the water from tank T2 back into tank T3, while pump P1 circulates the fresh water from tank T3 into tank T2. This allows continuous circulation of fresh water through the pipe systems. After the pipe system is cleaned, close the bypass section S4, switch off pump P1 and circulate the water back into tank T3, using pump P2. Both pumps are switched off. The remaining water in the pipe system is released by closing ball valve V7, lifting section S2 and opening the drainage valve D5.

**Values recorded in the CAFV/MAFV experiment:**

- 3 velocity values termed  $MAFV_{(A, 1, 2, 3)}$  for shape A.
- 3 velocity values termed  $MAFV_{(B, 1, 2, 3)}$  for shape B.
- 3 velocity values termed  $CAFV_{(A, 1, 2, 3)}$  for shape A.
- 3 velocity values termed  $CAFV_{(B, 1, 2, 3)}$  for shape B.

## 4.4 MTRV/MTSV - Experiment

### **MTRV/MTSV – Measured Parameter Definition:**

The task schedule of the *MTRV/MTSV - Experiment* is similar to the *CAFV/MAFV - Experiment*, but with help of this experiment, the minimum necessary velocity for a certain selected flow pattern is determined. The first determined parameter is the “*Minimum Transport Suspension Velocity*”. At the MTSV value no cuttings settle out of the drilling fluid. Solids and liquid are transported in suspension through the annular section of the flow loop. This would be the most favourable mode of transportation, but hardly achievable especially in extended-reach wells with long horizontal sections, due to the present force distributions acting on the solids, described in chapter 2.1.

The second determined value in this experiment is the “*Minimum Transport Rolling Velocity*”, which is defined to be the necessary velocity to ensure a moving cutting bed. No stationary bed can be observed, in contrast to the CAFV value. To identify the solids flow behaviour the measuring section in section S2 is used.

Contrary to the *CAFV/MAFV - Experiment*, the *MTRV/MTSV - Experiment* does not determine a velocity range, providing a minimum and a maximum value for desired modes of transportation. The obtained values in this experiment define the absolute minimum velocities to achieve a certain desired flow pattern, like “only moving bed” and “only suspension flow”.

Figure 4.5 shows the flow pattern achieved when the MTRV is applied.

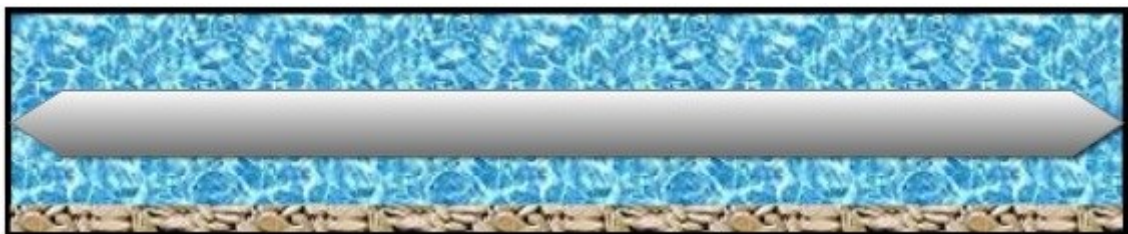


**Figure 4.5: Moving Cutting Bed**

The MTSV cause a flow pattern similar to the one of the MAFV. All solids maintain in suspension and no accumulation of cuttings can be observed.

**Experiment step by step implementation:**

**Step 1:** First step for the implementation of the MTRV/MTSV experiment is to agitate the drilling fluid at high velocity with help of the high revolution agitator E1 in mud tank T1 to ensure proper mud conditioning. The transparent pipe is in horizontal position, simulating a horizontal well section. In this stage both pumps are switched off. The ball valves V7 and V8 are open, while V6, V5, V3 and V1 are closed.

**Step 2:** After mud conditioning, the artificial cuttings shape A are added to the drilling fluid in mud tank T1. The stirring continues for another 5 minutes within the tank to provide a uniform solid distribution.

**Step 3:** Then pump P1 is used to circulate the suspension from mud tank T1 through the annular pipe section S2 into mud tank T2. The flow rate is selected to provide sufficient velocity to keep the solids in suspension and avoid settling and deposition on the lower side of the annular area. Therefore choose a flow rate slightly beneath the MAFV value to achieve laminar flow conditions and reduce it step by step until the minimum necessary annular velocity is reached to maintain the cuttings in suspension. If deposition of particles can be observed, the velocity is slightly increased again as long as all particles are in suspension. The transport behavior of the solids is observed in the measurement section in the middle of the transparent pipe. The minimum flow rate, that ensures suspension flow is recorded and converted to an annular velocity in the transparent pipe. Pump P2 is used to refill tank T1 in case that the liquid level in tank T1 is not sufficient to complete the experiment.

**Step 4:** To convert the flow rate into an annular velocity equations (49), (51) and (52) are used. The computed velocity represents the MTSV value.

**Step 5:** A further reduction of the flow rate causes the solids to drop out of the fluid and to accumulate on the lower side of the annulus, forming a moving cutting bed. An additional reduction would provoke the appearance of a stationary cutting bed. The flow rate is recorded, at which all cuttings are sliding on the bottom of the annulus and no stationary behavior can be observed.

**Step 6:** The recorded flow rate is converted into velocity units using equation (49), (51) and (52). The calculated velocity represents the MTRV value of cutting shape A.

**Step 7:** Last procedure is to increase the flow rate of pump P1 to its maximum to bring the deposited cuttings back into suspension and erode the formed cutting beds. At the same time switch on pump P2 and circulate the suspension back to mud tank T1. Using both pumps simultaneously allows permanent circulation through the pipe system. To avoid deposition of solids in tank T2 the bypass section S4 is used.

**Step 8:** To ensure the received values are meaningful and reproducible, repeat step 1 to 8 another two times for shape A.

**Step 9:** After determining three values for the MTSV and the MTRV for the first cutting shape, the solids are removed from the liquid. Therefore a sieve E5 is installed at tank T2. Pump P1 and P2 are used to provide permanent circulation through the pipe system, until no cuttings are collected anymore at the sieve. A high flow rate is chosen to establish turbulent flow and to whirl up deposited solids in the pipe system. Bypass section S4 is used to implement a radial velocity in tank T2 to remove cuttings from the bottom and corners. When no more cuttings are retrieved at the sieve, pump P1 is switched off and the sieve with the collected solids is removed.

**Step 10:** Repeat step 2 to 9, for cuttings shape B.

**Step 11:** To clean the pipe system evacuate the drilling fluid from tank T2 by switching off pump P1. Pump P2 is used to circulate the remaining drilling fluid back into mud tank T1. The dead volume of tank T2 is released with help of the

drain valve D2. The ball valves V6, V4, V3, and V2 are closed, while valve V5, V1 and V9 are opened. Then switch the pump P1 into tank T3, which is filled with fresh water and circulate at high velocity through the pipe system into mud tank T2. Pump P2 is used to circulate the water from tank T2 back into tank T3, while pump P1 circulates the fresh water from tank T3 into tank T2. This allows continuous circulation of fresh water through the pipe systems. After the pipe system is cleaned, close the bypass section S4, switch off pump P1 and circulate the water back into tank T3, using pump P2. Both pumps are switched off. The remaining water in the pipe system is released by closing ball valve V7, lifting section S2 and opening the drainage valve D5.

**Values recorded in the MTRV/MTSV - Experiment:**

- 3 velocity values called  $MTRV_{(A, 1, 2, 3)}$  for shape A.
- 3 velocity values called  $MTRV_{(B, 1, 2, 3)}$  for shape B.
- 3 velocity values called  $MTSV_{(A, 1, 2, 3)}$  for shape A.
- 3 velocity values called  $MTSV_{(B, 1, 2, 3)}$  for shape B.

## **4.5 CBH - Experiment**

**CBH - Measured Parameter Definition:**

An essential information, for controlling bottom-hole pressure, minimize circulation time for wellbore cleaning and prevent pipe sticking, is the amount of cuttings that deposited and accumulated in the horizontal and highly-inclined wellbore sections. Therefore a common parameter used for estimation of cutting transport efficiency and accumulation tendency is the bed height of the solids accumulated on the lower side of the annular area.



There is no direct measurement of the cutting bed height, but an excessive increase can be recognised due to increasing torque and drag readings on surface. Since more area of the DP is buried in deposited cuttings, a higher torque and drag force is necessary to rotate or actuate the drill pipe against the friction and weight forces of the solids acting on the pipe. An excessive bed height also increases the risk of stuck pipe tendency dramatically. During drilling operations, an increase or a critical level of cuttings bed height can only be recognised by observing the power consumption of the top drive due to an increased required torque.

In the cutting bed height experiment, simply put *CBH - Experiment*, the height of the stationary bed is determined by measuring the perimeter of the transparent pipe that is occupied with deposited solids. The measured perimeter values are then converted to bed heights with equation (56) and (57).

$$B = \frac{2 r \pi \alpha}{360} \quad (56)$$

$$\cos \alpha = \frac{A}{r} \quad (57)$$

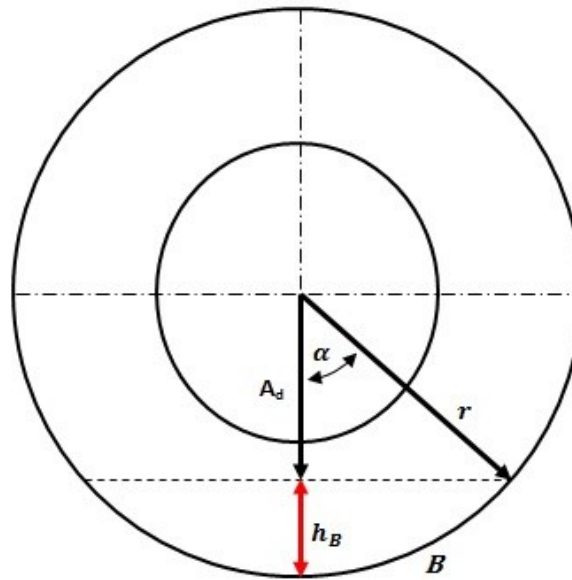


Figure 4.6: Cuttings Bed Perimeter

$B$  ... Arc length  
 $h_B$  ... Height of Bed  
 $\alpha$  ... Angle  
 $A_d$  ... Adjacent  
 $r$  ... Radius (Hypotenuse)

**Experiment step by step implementation:**

**Step 1:** First step of the CBH experiment is to agitate the drilling fluid at high velocity with help of the high revolution agitator E1 in mud tank T1 to ensure proper mud conditioning. The transparent pipe is in horizontal position, simulating a horizontal well section. In this stage both pumps are switched off. The ball valves V7 and V8 are open, while V6, V5, V3 and V1 are closed.

**Step 2:** Then the artificial cuttings are added to the drilling fluid in mud tank T1, starting with shape A. The slurry is circulated within the tank for another 5 minutes to ensure proper stirring and a uniform solids distribution.

**Step 3:** Next step is to switch on pump P1 and circulate the suspension at high velocity through the annular section into mud tank number T2. After filling up the whole pipe system, the flow rate is reduced to the lowest value that allows the

cuttings to accumulate on the lower side of the annulus, which is represented by the CAFV value. This fluid velocity provokes the formation of a stationary cutting bed. The CAFV value has been determined in the CAFV/MAFV experiment. After the shape dependent CAFV value has been chosen, solids start to settle out of the suspension and deposit on the lower side of the annulus, forming a stationary cutting bed. For shape A the  $CAFV_{(A)}$  value is chosen and for shape B the  $CAFV_{(B)}$  value is chosen.

**Step 4:** After a predefined time of circulation an image of the measuring section in the transparent pipe section S2 is taken. With help of the scale unit at the beginning and the end of the control section the stationary bed perimeter can be determined. The bed perimeter is then converted into a cutting bed height with the equations (56) and (57).

**Step 5:** After an image of the cuttings bed has been taken, the flow rate of pump P1 is increased to the maximum to flush all deposited solids out of the pipe into tank T2. At the same time, pump P2 is switched on and the suspension is circulated back into mud tank T1. After the cutting bed in the transparent pipe section is eroded, the loop system is ready to continue with step 6.

**Step 6:** To ensure the received values are meaningful and reproducible, step 1 to 5 is repeated further two times for shape A.

**Step 7:** After the last round of the experiment the cuttings shape A are removed from the drilling fluid. Therefore a sieve E5 is installed at tank T2. Pump P1 and P2 are used to provide permanent circulation through the pipe system, until no cuttings are collected anymore at the sieve. A high flow rate is chosen to establish turbulent flow and to whirl up deposited solids in the pipe system. Bypass section S4 is used to implement a radial velocity in tank T2 to remove cuttings from the bottom and corners. When no more cuttings are retrieved at the sieve, pump P1 is switched off and the sieve with the collected solids is removed.

**Step 8:** Step 2 to 7 is repeated with cuttings shape B.

**Step 9:** To clean the pipe system the drilling fluid is evacuated from tank T2 by switching off pump P1. Pump P2 is used to circulate the remaining drilling fluid back into mud tank T1. The dead volume of tank T2 is released with help of the drain valve D2. The ball valves V6, V4, V3, and V2 are closed, while valve V5, V1 and V9 are opened. Pump P1 is switched into tank T3, which is filled with fresh water and circulate at high velocity through the pipe system into mud tank T2. Pump P2 is used to circulate the water from tank T2 back into tank T3, while pump P1 circulates the fresh water from tank T3 into tank T2. This allows continuous circulation of fresh water through the pipe systems. After the pipe system is cleaned, close the bypass section S4, switch off pump P1 and circulate the water back into tank T3, using pump P2. Both pumps are switched off. The remaining water in the pipe system is released by closing ball valve V7, lifting section S2 and opening the drainage valve D5.

**Values recorded in the CBH - Experiment:**

- 3 height values termed  $CBH_{(A, 1, 2, 3)}$  for shape A.
- 3 height values termed  $CBH_{(B, 1, 2, 3)}$  for shape B.

## **4.6 CBET - Experiment**

**CBET - Measured Parameter Definition:**

In case of a circulation stop, the cuttings settle out of the drilling fluid and deposit on the lower side of the annulus in the wellbore, forming a stationary cutting bed, which might cause severe problems in the drilling process. To avoid immediate settling of solids out of the fluid, drilling muds are designed to create a gel strength, which decelerates the cuttings settling velocity in case of stopped circulation. There are many reasons why a circulation stop is performed, for example a flow check for kick detection, making or breaking of connections,

maintenance work, stuck pipe or when a stand pipe pressure increase is observed at the surface. The shape of the cuttings also influences the consolidation and stabilisation of the formed cutting bed. Therefore a different momentum force of the fluid is necessary to withdraw the deposited solids and convert a stationary cutting bed to a moving cutting bed.

For that reason the time, which is necessary to withdraw the stationary cutting bed with a predefined velocity is determined in the *Cuttings Bed Erosion Time Experiment* for both previously described cutting shapes.

### **Experiment step by step implementation:**

**Step 1:** First step of the *CBET - Experiment* is to agitate the drilling fluid at high velocity with help of the high revolution agitator E1 in mud tank T1 to ensure proper mud conditioning. The transparent pipe is in horizontal position, simulating a horizontal wellbore section. In this stage both pumps are switched off. The ball valves V7 and V8 are open, while V6, V5, V3 and V1 are closed.

**Step 2:** The artificial cuttings are added into the drilling fluid in mud tank T1, starting with shape A. The slurry is circulated within the tank for another 5 minutes to ensure proper stirring and a uniform solids distribution.

**Step 3:** The flow rate, which corresponds the MTSV value for the respective solid shape is chosen to ensure all cuttings are in suspension as being circulated through the cutting transport simulation apparatus. When the whole pipe system is filled up, the mud pump P1 is switched off, causing a circulation stop in the transparent pipe. This allows the solids to settle and deposit on the lower side of the annulus forming a cutting bed. Since the MTSV value for the respective cutting shape is chosen as starting flow rate, the cutting bed perimeter observed in the transparent pipe section should be equal for both shapes. If not, circulation is continued with the CAFV value allowing further solids to deposit in section S2 until the bed perimeter is the same.

**Step 4:** Mud pump P1 is switched from tank T1 into tank T4, which is filled with pure drilling fluid. The three way ball valve B4 with a “T” hole inside is actuated and valve V10 is opened to allow circulation through bypass section S5. Pump P1 is switched on and stirs the drilling fluid in mud tank T4 to break up the fluids gel strength. Before actuating valve B4 again and closing valve V10 to allow the drilling fluid to flow through section S1 and start eroding the deposited solids in section S2, choose the flow rate which represents the MTRV. This value should represent the flow rate causing a fluid momentum high enough to lift the cuttings off the ground and convert the stationary cutting bed into a moving cutting bed. The time is measured from the point in time when the three way ball valve B4 is actuated the second time, allowing circulation through the transparent pipe section, using the MTRV flow rate, until the last solid leaves the transparent pipe section S2.

**Step 5:** After measuring the time necessary to remove the stationary cutting bed, the sieve E5 is installed on tank T2 and the flow rate of pump P1, still positioned in tank T4, is increased to the maximum to flush all deposited solids out of the pipe system into tank T2. During this experiment the fluid level in mud tank T2 needs to be observed very accurately, since suspension and fluid is pumped from tank T1 and tank T4, the capacity of tank T2 might not be sufficient, depending on the necessary duration of circulation to erode the formed cutting bed. If a critical level in tank T2 is reached pump P1 is switched off. Sieve E5 is installed on tank T4 to separate the solids from the drilling fluid. The ball valve V3 is opened while V2 is closed and pump P2 is switched on to refill tank T4. To remove deposited solids in tank T2, the bypass section S4 is used. The solids collected in the sieve are added again to tank T1. After filling up tank T4, pump P1 is switched back into tank T1 and valve V3 is closed, while V2 is opened to refill tank T1 again. Now tank T4 is filled again with pure drilling fluid and tank T1 contains the suspension of solids and drilling fluid.

**Step 6:** To ensure the received values are meaningful and reproducible, repeat step 2 to 5 further two times for shape A.

**Step 7:** After determining three time values for cutting shape A, the solids are removed from the liquid. Therefore a sieve E5 is installed at tank T2. Pump P1 and P2 are used to provide permanent circulation through the pipe system, until no cuttings are collected anymore at the sieve. A high flow rate is chosen to establish turbulent flow and to whirl up deposited solids in the pipe system. Bypass section S4 is used to implement a radial velocity in tank T2 to remove cuttings from the bottom and corners. When no more cuttings are retrieved at the sieve, pump P1 is switched off and the sieve with the collected solids is removed.

**Step 8:** Repeat step 2 to 7, with cuttings shape B.

**Step 9:** To clean the pipe system evacuate the drilling fluid from tank T2 by switching off pump P1. Pump P2 is used to circulate the remaining drilling fluid back into mud tank T1. The dead volume of tank T2 is released with help of the drain valve D2. The ball valves V6, V4, V3, and V2 are closed, while valve V5, V1 and V9 are opened. Then switch the pump P1 into tank T3, which is filled with fresh water and circulate at high velocity through the pipe system into mud tank T2. Pump P2 is used to circulate the water from tank T2 back into tank T3, while pump P1 circulates the fresh water from tank T3 into tank T2. This allows continuous circulation of fresh water through the pipe systems. After the pipe system is cleaned, close the bypass section S4, switch off pump P1 and circulate the water back into tank T3, using pump P2. Both pumps are switched off. The remaining water in the pipe system is released by closing ball valve V7, lifting section S2 and opening the drainage valve D5.

**Values recorded in the CBET - Experiment:**

- 3 time values termed  $CBET_{(A, 1, 2, 3)}$  for shape A.
- 3 time values termed  $CBET_{(B, 1, 2, 3)}$  for shape B.

## 4.7 SV - Experiment

According to Sample *et al.* (1978) cutting settling velocities, determined in static drilling fluids, which are generally non-Newtonian, provide more accurate results for the cutting slip velocity than any of the previously mentioned slip velocity correlations [29].

Therefore the settling velocity of both cutting shapes is additionally measured in the laboratory under static conditions. Therefore a transparent cylinder is filled with the proposed transparent drilling fluid and the time necessary for the particles to travel from top of the fluid level to the bottom of the cylinder is measured. The drilling fluid rheology is described in chapter 3.2. To observe also the influence of the interaction of the cuttings shape and the limiting wall, the inclination of the cylinder is changed from 0 to 45 degree from vertical.

Equation (48) is used to calculate the settling velocity of the solid with help of the measured time and the travelled distance.

### **Values recorded in the SV - Experiment:**

- 3 time values termed  $SV_{(A, 1, 2, 3)}$  for shape A with 0 degree inclination and 3 time values termed  $SV_{(A, 1.1, 2.1, 3.1)}$  with 45 degree inclination.
- 3 time values termed  $SV_{(B, 1, 2, 3)}$  for shape B with 0 degree inclination and 3 time values termed  $SV_{(B, 1, 2, 3)}$  with 45 degree inclination.

## 4.8 MASV - Experiment

The velocity value determined in the *MASV - Experiment* has the same magnitude as the velocity determined in the *MTRV/MTSV - Experiment*, the *Minimum Transport Suspension Velocity* (MTSV). It represents the minimum velocity necessary in the annular section to keep the cuttings in suspension and to avoid



settling or accumulation of solids on the bottom of the wellbore. Therefore it is called *Minimum Annular Suspension Velocity* (MASV). However the method of determination is different from the *MTRV/MTSV - Experiment* and allows for a comparison between the velocities determined in the experiments. The implementation of the *MASV - Experiment* is a combination of the *CBH - Experiment* and the *MTRV/MTSV - Experiment*, since the bed perimeter is used to calculate the velocity to maintain suspension flow.

### **Experiment step by step implementation:**

**Step 1:** First step of the *MASV - Experiment* is to agitate the drilling fluid at high velocity with help of the high revolution agitator E1 in mud tank T1 to ensure proper mud conditioning. The transparent pipe is in horizontal position, simulating a horizontal well section. In this stage both pumps are switched off. The ball valves V7 and V8 are open, while V6, V5, V3 and V1 are closed.

**Step 2:** Then the artificial cuttings are added to the drilling fluid in mud tank T1, starting with shape A. The slurry is circulated within the tank for another 5 minutes to ensure proper stirring and a uniform solids distribution.

**Step 3:** Next step is to switch on pump P1 and circulate the suspension at high velocity through the annular section into mud tank number T2. After filling up the whole pipe system, the flow rate is reduced to the lowest value that allows the cuttings to accumulate on the lower side of the annulus, which is represented by the CAFV value. This fluid velocity provokes the formation of a stationary cutting bed. The CAFV value has been determined in the *CAFV/MAFV - Experiment*. After the shape dependent CAFV value has been chosen, solids start to settle out of the suspension and deposit on the lower side of the annulus, forming a stationary cutting bed. For shape A the  $CAFV_{(A)}$  value is chosen and for shape B the  $CAFV_{(B)}$  value is chosen.

**Step 4:** After a cutting bed has formed, the mass flow reading of the second coriolis mass flow meter is observed. Since at the beginning the cutting bed in the annular

area is not fully developed, the mass inflow reading at the first mass flow meter E8 is higher than the mass outflow reading seen at the second mass flow meter E9. Once the cutting bed is stable, both readings will be equal and the cutting bed perimeter is determined in the same way as described in the *CBH – Experiment*. Then the remaining annular open flow area is determined by subtracting the occupied area from the cross-sectional area of the transparent pipe and by subtracting the cross-sectional area of the simulated drill pipe. The remaining area represents the open flow area and due to the decrease of the open flow area, the annular velocity is increased until the MASV is reached and the solid particles are kept in suspension while travelling through the transparent pipe section S2. Equation (51) is used to convert the flow rate and the determined open flow area into a MASV value, which can then be compared with the MTSV value.

**Step 5:** After the MASV value is determined, the flow rate of pump P1 is increased to the maximum to flush all deposited solids out of the pipe into tank T2. At the same time pump P2 is switched on and the suspension is circulated back into mud tank T1. After the cutting bed in the transparent pipe section is eroded, the loop system is ready to continue with step 6.

**Step 6:** To ensure the received values are meaningful and reproducible, step 1 to 5 is repeated further two times for shape A.

**Step 7:** After the last round of the experiment the cuttings shape A are removed from the drilling fluid. Therefore a sieve E5 is installed at tank T2. Pump P1 and P2 are used to provide permanent circulation through the pipe system, until no cuttings are collected anymore at the sieve. A high flow rate is chosen to establish turbulent flow and to whirl up deposited solids in the pipe system. Bypass section S4 is used to implement a radial velocity in tank T2 to remove cuttings from the bottom and corners. When no more cuttings are retrieved at the sieve, pump P1 is switched off and the sieve with the collected solids is removed.

**Step 8:** Step 2 to 7 is repeated with cuttings shape B.

**Step 9:** To clean the pipe system the drilling fluid is evacuated from tank T2 by switching off pump P1. Pump P2 is used to circulate the remaining drilling fluid

back into mud tank T1. The dead volume of tank T2 is released with help of the drain valve D2. The ball valves V6, V4, V3, and V2 are closed, while valve V5, V1 and V9 are opened. Pump P1 is switched into tank T3, which is filled with fresh water and circulate at high velocity through the pipe system into mud tank T2. Pump P2 is used to circulate the water from tank T2 back into tank T3, while pump P1 circulates the fresh water from tank T3 into tank T2. This allows continuous circulation of fresh water through the pipe systems. After the pipe system is cleaned, close the bypass section S4, switch off pump P1 and circulate the water back into tank T3, using pump P2. Both pumps are switched off. The remaining water in the pipe system is released by closing ball valve V7, lifting section S2 and opening the drainage valve D5.

**Values recorded in the MASV - Experiment:**

- 3 velocity values called  $MASV_{(A, 1, 2, 3)}$  for shape A.
- 3 velocity values called  $MASV_{(B, 1, 2, 3)}$  for shape B.

## 5 CONCLUSION

The first objective, to develop and implement experiments to investigate the impact of the cuttings shape on removal, transportation and accumulation characteristics was only partly fulfilled. Experiments were defined and could be presented in this thesis, which can be used to produce meaningful results. However the existing flow loop presented in the introduction, proved not to be suitable for the proposed tests. Therefore it was decided to design a new flow loop for teaching purposes and experimental investigations. The proposed tests about the impact of the cuttings shape could not be conducted in the course of this thesis, but a new design concept of a cutting transport simulation apparatus with the necessary prerequisites and the necessary additional equipment could be developed and the apparatus will be built in the future. The new design concept enables the investigation of various parameters influencing cutting transport efficiency and accumulation tendencies. Besides the cutting shape, additional factors as changing inclination, *Rate of Penetration* (ROP), density effects, the impact of gas inflow and aerated drilling fluids can be investigated.

Performing the developed experiments and investigating the previously mentioned parameters to evaluate the cutting shape influence on transport and accumulation characteristics, bridge an important gap in the understanding of solid transportation and hole cleaning, which helps to improve the overall drilling process. Health, safety and environmental risks are reduced and even profits may increase, due to lower costs and less unexpected problems related to poor cutting removal and hole cleaning. Improved solids removal and cutting transportation increase the lifetime of a drill bit, increase the ROP and help to maintain the *Equivalent Circulation Density* (ECD) within the mud weight window, which avoids unplanned fracturing of the formation and furthermore excessive torque and drag, which possibly leads to mechanical pipe sticking.

Furthermore the gained results from the experiments can provide the possibility to modify formerly derived slip velocity correlations, which help to predict, estimate and calculate hole cleaning efficiency more accurately.

Generally, an improved understanding of the parameters influencing cutting transportation in the different sections of a wellbore, leads to an optimization of the drilling process. Knowing the advantages or disadvantages of either the one or the other shape of solids may help to adjust drilling parameters and procedures to face these days challenges, like increased horizontal departures and depths.

## 6 FUTURE WORK

A future work recommendation is to investigate the impact of drilling parameters on the cutting shape. It might be possible to generate a desired solid shape by adjusting drilling parameters like the *Revolutions per Minute* (RPM), *Weight on Bit* (WOB) and the *Depth of Cut* (DOC). In case a desired shape can be generated, it would also be necessary to find out, if the shape of the cuttings can be maintained while travelling upwards through the annulus?

Furthermore it is recommended to produce additional sizes of the previously described shapes of cuttings and compare the gained results for non-uniform solid size distribution.

For more meaningful results, it might be useful to implement a curved transparent pipe instead of the straight pipe, to simulate cutting transportation in the most critical section of a wellbore, the build section.

# NOMENCLATURE

## List of Abbreviations

AFV	Annular Flow Velocity	MAFV	Maximum Annular Flow Velocity
ANN	Artificial Neural Network	MASV	Minimum Annular Suspension Velocity
API	American Petroleum Institute	MD	Measured Depth
BHA	Bottom-Hole Assembly	MTRV	Minimum Transport Rolling Velocity
CAFV	Critical Annular Flow Velocity	MTSV	Minimum Transport Suspension Velocity
CBET	Cutting Bed Erosion Time	MTV	Minimum Transport Velocity
CBH	Cuttings Bed Height	OD	Outside Diameter
CTV	Critical Transport Velocity	OFA	Open Flow Area
DOC	Depth of Cut	PDC	Polycrystalline Diamond Compound
DP	Drill Pipe	PV	Plastic Viscosity
ECD	Equivalent Circulating Density	ROP	Rate of Penetration
ERD	Extended Reach Drilling	RPM	Revolutions per Minute
HP	Horsepower	SI	Système International d'Unités
HSE	Health Safety and Environmental	SV	Settling Velocity
IBC	Intermediate Bulk Container	TV	Transport Velocity
ID	Inside Diameter	WOB	Weight on Bit
LPAT	Low Pressure Ambient Temperature	YP	Yield Point

## List of Symbols

- $A$  = cross-sectional area,  $m^2$  or  $ft^2$   
 $A_d$  = adjacent, m  
 $A_m$  = cross-sectional area of the model,  $m^2$   
 $A_p$  = cross-sectional area of the prototype,  $m^2$   
 $A_o$  = open flow cross-sectional area,  $m^2$   
 $A_w$  = cross-sectional wellbore area,  $m^2$   
 $B$  = arc length, m  
 $C$  = volumetric concentration, dimensionless  
 $d_s$  = diameter of particle, inch  
 $d_1$  = outside diameter of inner pipe, m or in  
 $d_2$  = inside diameter of outer pipe, m or in  
 $f$  = Fanning friction factor, dimensionless  
 $F_T$  = cutting transport ratio, percent  
 $g$  = gravitational acceleration,  $m/s^2$   
 $h$  = thickness of particle, in  
 $h_B$  = height of bed, m  
 $h_o, h_1$  = geodätic height at entrance and middle of venturi pipe, m  
 $K$  = consistency index, cp or  $Pa \cdot s$   
 $L_m$  = clearance of the model, m  
 $L_p$  = clearance of the prototype, m  
 $m$  = mass flow,  $kg/s$   
 $n$  = flow index, dimensionless  
 $N$  = rotary speed of viscometer, rpm  
 $N_{Re}$  = Reynolds number, dimensionless  
 $N_{ReC}$  = critical Reynolds number, dimensionless  
 $p$  = pressure, Pa  
 $P_o, P_1$  = pressure at entrance and middle of venturi pipe, Pa  
 $q$  = flow rate,  $m^3/s$  or gpm  
 $Q$  = flow rate,  $m^3/s$  or gpm  
 $Q_{inj}$  = injection rate,  $m^3/s$   
 $r$  = radius, m  
 $s$  = distance between detectors, m  
 $s_o$  = open flow wetted perimeter, m  
 $t$  = time, s  
 $u$  = velocity,  $m/s$   
 $v$  = average flow velocity,  $m/s$  or  $ft/s$   
 $v_a$  = annular velocity of fluid,  $m/s$   
 $v_{sl}$  = particle slip velocity,  $m/s$   
 $v_T$  = cutting transport velocity,  $m/s$   
 $v_o, v_1$  = velocities at entrance and middle of venturi pipe,  $m/s$   
 $V$  = volume flow,  $m^3/s$   
 $x$  = distance along horizontal well, m  
 $\Delta s$  = change of mass between layers,  $kg/s \cdot m^3$



**□Greek Symbols**

$\alpha$  = angle

$\beta_v$  = drag force coefficient, kg/(s\*m<sup>2</sup>)

$\dot{\gamma}_s$  = shear rate, s<sup>-1</sup>

$\Theta_N$  = dial reading of viscometer at rotary speed N, lbf/100ft<sup>2</sup> or Pa

$\mu$  = viscosity, cp or Pa\*s

$\mu_a$  = apparent viscosity, cp or Pa\*s

$\mu_p$  = plastic viscosity, cp or Pa\*s

$\rho$  = density, kg/m<sup>3</sup>

$\rho_f$  = fluid density, kg/m<sup>3</sup> or ppg

$\rho_s$  = solid density, kg/m<sup>3</sup> or ppg

$\tau_s$  = shear stress, lbf/100ft<sup>2</sup> or Pa

$\tau_y$  = yield point, lbf/100ft<sup>2</sup> or Pa

**□Subscripts**

1,2 = two points of interest in the flow loop

*f* = fluid

*s* = solid

*A* = Shape A

*B* = Shape B

## SI METRIC CONVERSION FACTORS

bbbl	×	1.589 873	E-01	=	m <sup>3</sup>
cp	×	1.0*	E-03	=	Pa·s
ft	×	3.048*	E-01	=	m
ft-lbs	×	1.355 818	E+00	=	Nm
ft/min	×	5.080*	E-03	=	m·s <sup>-1</sup>
°F	×	(°F - 32)/1.8		=	°C
°F	×	(°F + 459.67)/1.8		=	K
U.S. gal	×	3.785 412	E-03	=	m <sup>3</sup>
hp	×	7.456 999	E+02	=	W
in.	×	2.54*	E-02	=	m
lb <sub>f</sub>	×	4.448 222	E+00	=	N
lb <sub>m</sub>	×	4.535 924	E-01	=	kg
lb <sub>m</sub> /ft	×	1.488 164	E+00	=	kg·m <sup>-1</sup>
psi	×	6.894 757	E+03	=	Pa
psi/ft	×	2.262 059	E+04	=	Pa·m <sup>-1</sup>
ppg	×	1.198 264	E+02	=	kg·m <sup>-3</sup>

\*Conversion factor is exact

## REFERENCES

- [1] Baker Hughes, “Drilling Fluids Reference Manual,” in *Hydraulics*, 2006, p. 502.
- [2] J. J. Azar and R. G. Samuel, “Drilling Engineering,” in *Transport of Drilled Cuttings*, Tulsa, Oklahoma, PennWell Corporation, ISBN 978-1-59370-072-0, 2007.
- [3] J. Haugen, “Oil & Gas Journal,” 03 February 1998. [Online]. Available: <http://www.ogj.com/articles/print/volume-96/issue-9/in-this-issue/general-interest/rotary-steerable-system-replaces-slide-mode-for-directional-drilling-applications.html>. [Accessed 07 January 2016].
- [4] M. Mohammadsalehi and N. Malekzadeh, *Optimization of Hole Cleaning and Cutting Removal in Vertical, Deviated and Horizontal Wells*, Prepared for Presentation at the SPE Asia Pacific Oil and Gas Conference and Exhibition in Jakarta, Indonesia: Society of Petroleum Engineers, SPE-143675, 2011.
- [5] R. G. Samuel and X. Liu, “Advanced Drilling Engineering,” in *Well Path Planning-2D*, Houston, Texas, Gulf Publishing Company, ISBN 978-1933762340, 2009, p. 153 .
- [6] R. B. Adari, S. Miska, E. Kuru, P. Bern and A. Saasen, *Selecting Drilling Fluid Properties and Flow Rates For Effective Hole Cleaning in High-Angle and Horizontal Wells*, Presented at Annual Technical Conference and Exhibition in Dallas, Texas: Society of Petroleum Engineers, SPE-63050, 2000.
- [7] B. Zohuri, “Dimensional Analysis and Self-Similarity Methods for Engineers and Scientists,” in *Similitude Theory and Applications*, Switzerland, Springer International Publishing, ISBN 978-3-319-13475-8, 2015, pp. 94-96 Vol.1.
- [8] G. L. Boyun Guo, “Applied Drilling Circulation Systems: hydraulics, calculations, and models,” in *Equipment in Mud Circulating*, Burlington, Massachusetts, Elsevier Inc., ISBN 978-0-12-381957-4, 2011, p. 4.
- [9] Mud Control Equipment, 2010. [Online]. Available: <http://www.mudcontrolequipment.com/pages/default.asp?p1=195>. [Accessed 26 January 2016].
- [10] C. J. Hopkins and R. A. Leicksenring, *Reducing the Risk of Stuck Pipe in the Netherlands*, Presented at the SPE/IADC Drilling Conference in Amsterdam: Society of Petroleum Engineers/ International Association of Drilling Contractors, SPE/IADC-29422, 1995.
- [11] R. F. Mitchell and S. Z. Miska, “Fundamentals of Drilling Engineering,” in *Drilling Hydraulics*, Richardson, Texas, Society of Petroleum Engineers, ISBN 978-1-55563-207-6, 2011, pp. SPE Textbook Series, Vol.12.
- [12] A. T. Bourgoyne Jr., K. K. Millheim, M. E. Chenevert and F. S. Young Jr., “Applied Drilling Engineering,” in *Drilling Hydraulics*, Richardson, Texas, Society of Petroleum Engineers, ISBN 978-1-55563-001-0, 1986, p. Vol.2.
- [13] T. I. Larsen, A. A. Pilehvari and J. J. Azar, *Development of a New Cuttings-Transport Model for High-Angle Wellbores Including Horizontal Wells*, Presented at the SPE Rocky Mountain Meeting/ Low Permeability Reservoirs Symposium in Denver, Colorado: Society of Petroleum Engineers, SPE-25872-PA, 1997.

- [14] N. B. Egenti, *Understanding Drill-Cuttings Transportation in Deviated and Horizontal Wells*, Prepared for Presentation at the SPE Nigeria Annual International Conference and Exhibition in Lagos, Nigeria: Society of Petroleum Engineers, SPE-172835-MS, 2014.
- [15] N. Malekzadeh and M. Mohammadsalehi, *Hole Cleaning Optimization in Horizontal Wells, a New Method to Compensate Negative Hole Inclination Effects*, Presented at Brasil Offshore Conference and Exhibition in Macae, Brazil: Society of Petroleum Engineers, SPE-143676, 2011.
- [16] P. H. Tomren, A. W. Iyoho and J. J. Azar, *Experimental Study of Cuttings Transport in Directional Wells*, Presented at the SPE Annual Technical Conference and Exhibition in San Francisco: Society of Petroleum Engineers, SPE-12123-PA, 1986.
- [17] American Petroleum Institute, "Rheology and hydraulics of oil-well drilling fluids," in *API Recommended Practice 13D*, Washington DC, American Petroleum Institute, Fifth edition, 2006.
- [18] T. R. Sifferman and T. E. Becker, *Hole Cleaning in Full-Scale Inclined Wellbores*, Presented at the SPE Annual Technical Conference and Exhibition in New Orleans: Society of Petroleum Engineers, SPE-20422-PA, 1992.
- [19] S. Naganawa, R. Sato and M. Ishikawa, *Cuttings Transport Simulation Combined With Large-Scale Flow Loop Experiment and LWD Data Enables Appropriate ECD Management and Hole Cleaning Evaluation in Extended-Reach Drilling*, Presented at International Petroleum Exhibition and Conference in Abu Dhabi, UAE: Society of Petroleum Engineers, SPE-171740-MS, 2014.
- [20] E. M. Ozbayoglu, S. Z. Miska, T. Reed and N. Takach, *Analysis of Bed Height in Horizontal and Highly-Inclined Wellbores by Using Artificial Neural Networks*, Presented at the SPE International Thermal Operations and Heavy Oil Symposium and International Horizontal Well Technology Conference in Calgary, Alberta: Society of Petroleum Engineers/ Petroleum Society of CIM/CHOA, SPE-78939, 2002.
- [21] A. A. Gavignet and I. J. Sobey, *A Model for the Transport of Cuttings in Highly Deviated Wells*, Presented at the SPE Annual Technical Conference and Exhibition in New Orleans, Louisiana: Society of Petroleum Engineers, SPE-15417, 1986.
- [22] Y. Masuda, Q. Doan, M. Oguztoreli, S. Naganawa, T. Yonezawa, A. Kobayashi and A. Kamp, *Critical Cuttings Transport Velocity in Inclined Annulus: Experimental Studies and Numerical Simulation*, Presented at the SPE/PS-CIM International Conference on Horizontal Well Technology in Calgary, Alberta: Society of Petroleum Engineers/Petroleum Society of CIM, SPE/PS-CIM 65502, 2000.
- [23] Y. Li, N. Bjorndalen and E. Kuru, *Numerical Modelling of Cuttings Transport in Horizontal Wells Using Conventional Drilling Fluids*, Presented at the 5th Canadian International Petroleum Conference, Calgary, Alberta: JCPT, Journal of Canadian Petroleum Technology, 2007.
- [24] D. Nguyen and S. S. Rahman, *A Three-Layer Hydraulic Program for Effective Cuttings Transport and Hole Cleaning in Highly Deviated and Horizontal Wells*, Society of Petroleum Engineers, SPE-51186, 1998.
- [25] H. Cho, N. Shah and S. O. Osisanaya, *A Three-Segment Hydraulic Model for Cuttings Transport in Horizontal and Deviated Wells*, Presented at the SPE/PS-CIM International Conference on Horizontal Well Technology in Calgary, Alberta: Society of Petroleum Engineers/Petroleum Society of CIM, SPE/PS-CIM 65488, 2000.
- [26] Z. Wang, Y. Zhai, X. Hao, X. Guo and L. Sun, *Numerical Simulation on Three Layer Dynamic Cutting Transport Model and Its Application on Extended Well Drilling*,

- Presented at the IADC/SPE Asia Pacific Drilling Technology Conference and Exhibition in Ho Chi Minh City, Vietnam: International Association of Drilling Contractors/ Society of Petroleum Engineers, IADC/SPE-134306, 2010.
- [27] A. L. Martins and C. C. Santana, *Evaluation of Cuttings Transport in Horizontal and Near Horizontal Wells - A Dimensionless Approach*, Presented at the Second Latin American Petroleum Engineering Conference in Caracas, Venezuela: Society of Petroleum Engineers, SPE-23643, 1992.
- [28] D. Nguyen and S. S. Rahman, *A Three-Layer Hydraulic Program for Effective Cuttings Transport and Hole Cleaning in Highly Deviated and Horizontal Wells*, Presented at IADC/SPE Asia Pacific Drilling Technology in Kuala Lumpur: Society of Petroleum Engineers, SPE-51186-PA, 1998.
- [29] K. J. Sample and A. T. Bourgoyne, *Development of Improved Laboratory and Field Procedures for Determining the Carrying Capacity of Drilling Fluids*, Presented at the SPE Annual Fall Technical Conference and Exhibition, Houston, Texas : Society of Petroleum Engineers, SPE-7497-MS, 1978.
- [30] E. G. Manger, *Porosity and Bulk Density of Sedimentary Rocks*, Washington D.C.: United States Government Printing Office, 1963.
- [31] DrillingFormulas.com, "DrillingFormulas.com," 14 February 2016. [Online]. Available: <http://www.drillingformulas.com/types-of-flow-and-rheology-models-of-drilling-mud/>. [Accessed 11 March 2016].
- [32] T. Nazari, G. Hareland and J. J. Azar, *Review of Cuttings Transport in Directional Well Drilling: Systematic Approach*, Presented at the SPE Western Regional Meeting in Anaheim, California: Society of Petroleum Engineers, SPE-132372, 2010.
- [33] S. Baldino, R. E. Osgouei, E. Ozbayoglu, S. Miska and N. Takach, *Cuttings Settling and Slip Velocity Evaluation in Synthetic Drilling Fluids*, Presented at the 12th Offshore Mediterranean Conference and Exhibition in Ravenna, Italy: Offshore Mediterranean Conference, OMC-2015-321, 2015.
- [34] C. E. Williams Jr. and G. H. Bruce, *Carrying Capacity of Drilling Muds*, Presented at the Fall Meeting of the Branch in New Orleans, Louisiana: Society of Petroleum Engineers, SPE-951111-G, 1951.
- [35] Drilling Contractor, "World's longest extended-reach well drilled offshore Qatar," *Drilling Contractor*, p. 14, July/August 2008.
- [36] K. Sonowal, B. Bennetzen, P. Wong and E. Isevcan, *How Continuous Improvement Led to the Longest Horizontal Well in the World*, Presented at IADC/SPE Drilling Conference and Exhibition, Amsterdam: International Association of Drilling Contractors/Society of Petroleum Engineers, IADC/SPE-119506, 2009.

